Exploring the Origin of the Rarest Stable Isotopes Naturally Occurring on Earth with Photon Beams

Adriana Banu

Department of Physics and Astronomy, James Madison University,
Harrisonburg, Virginia, USA

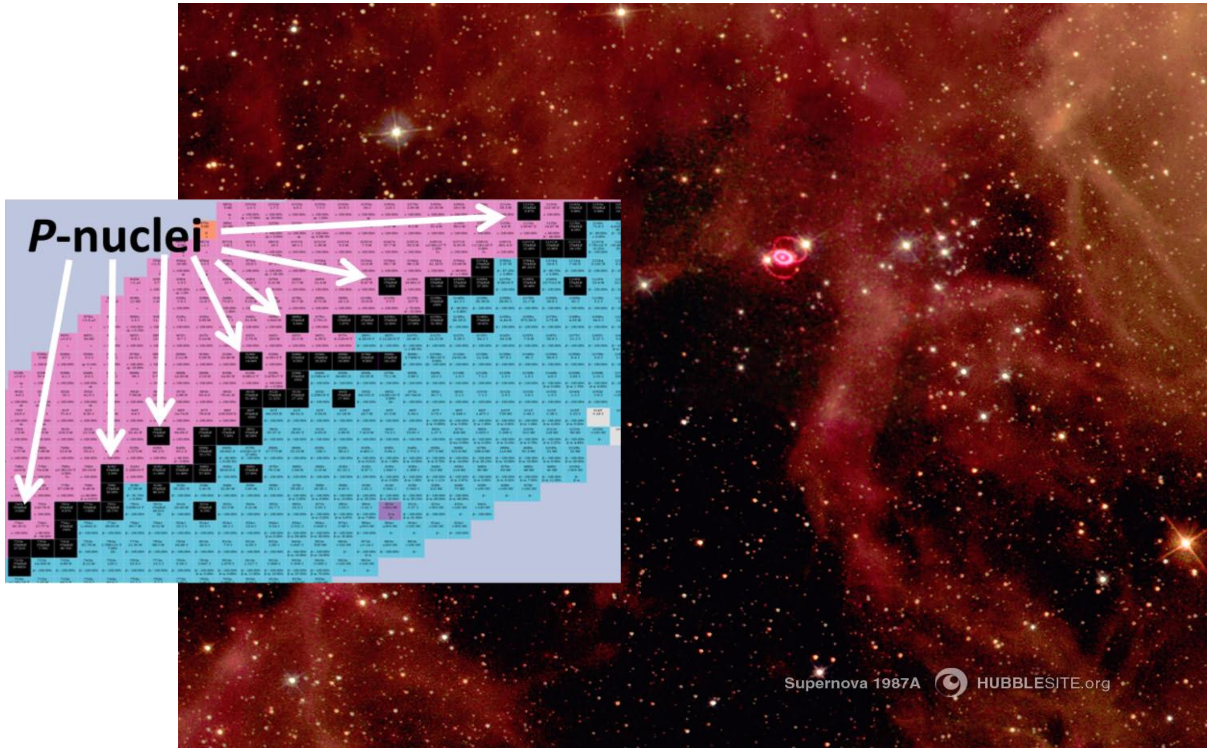

12th European Summer School on Experimental Nuclear Astrophysics
June 16-22, 2024, Aci Trezza, Catania, Italy

Collaborators:

A. M. Balbuena, R. L. Geissler, J. W. Goolsby, T. A. Hain, A. S. Kirk, E. G. Meekins, M. F. Mierisch, E. A. Witczak (all undergraduate students) & T. Pendleton – Madison Accelerator Lab Manager
James Madison University, Department of Physics and Astronomy

U. Friman-Gayer(*), S. W. Finch, R. V. F. Janssens, C. R. Howel, H. J. Karwowski *et al.*
Triangle Universities Nuclear Laboratory (TUNL)
Duke University, University of North Carolina at Chapel Hill
(*) currently at European Spallation Source ERIC, Sweden

J.A. Silano
Nuclear and Chemical Sciences Division
Lawrence Livermore National Laboratory

S. Goriely
Institut d'Astronomie et d'Astrophysique (IAA)
Université Libre de Bruxelles

The *p*-process is responsible for the nucleosynthesis beyond iron of ~35 proton-rich stable nuclei

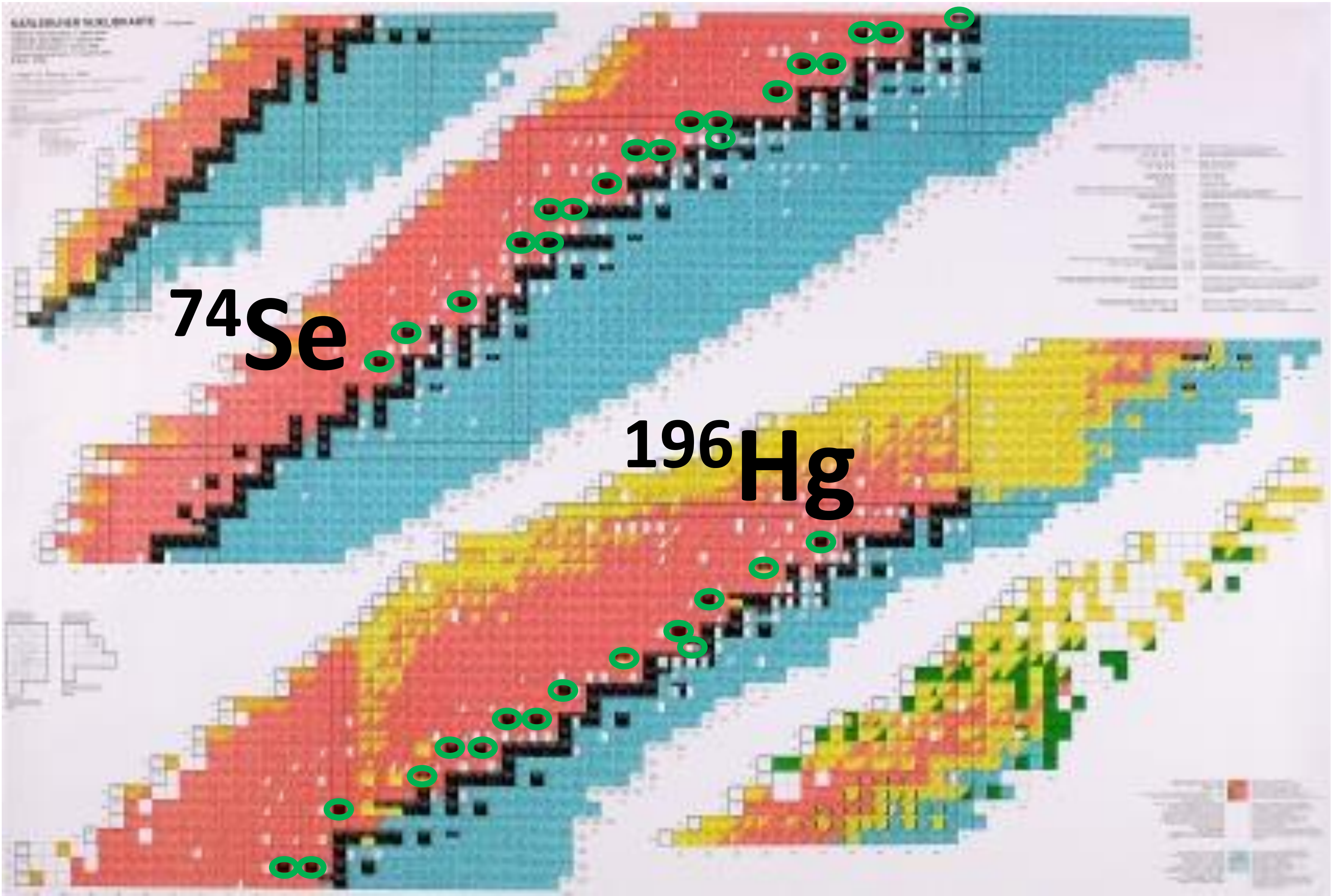

The *p*-Nuclei - ‘nuclear astrophysics *p*-nuts’

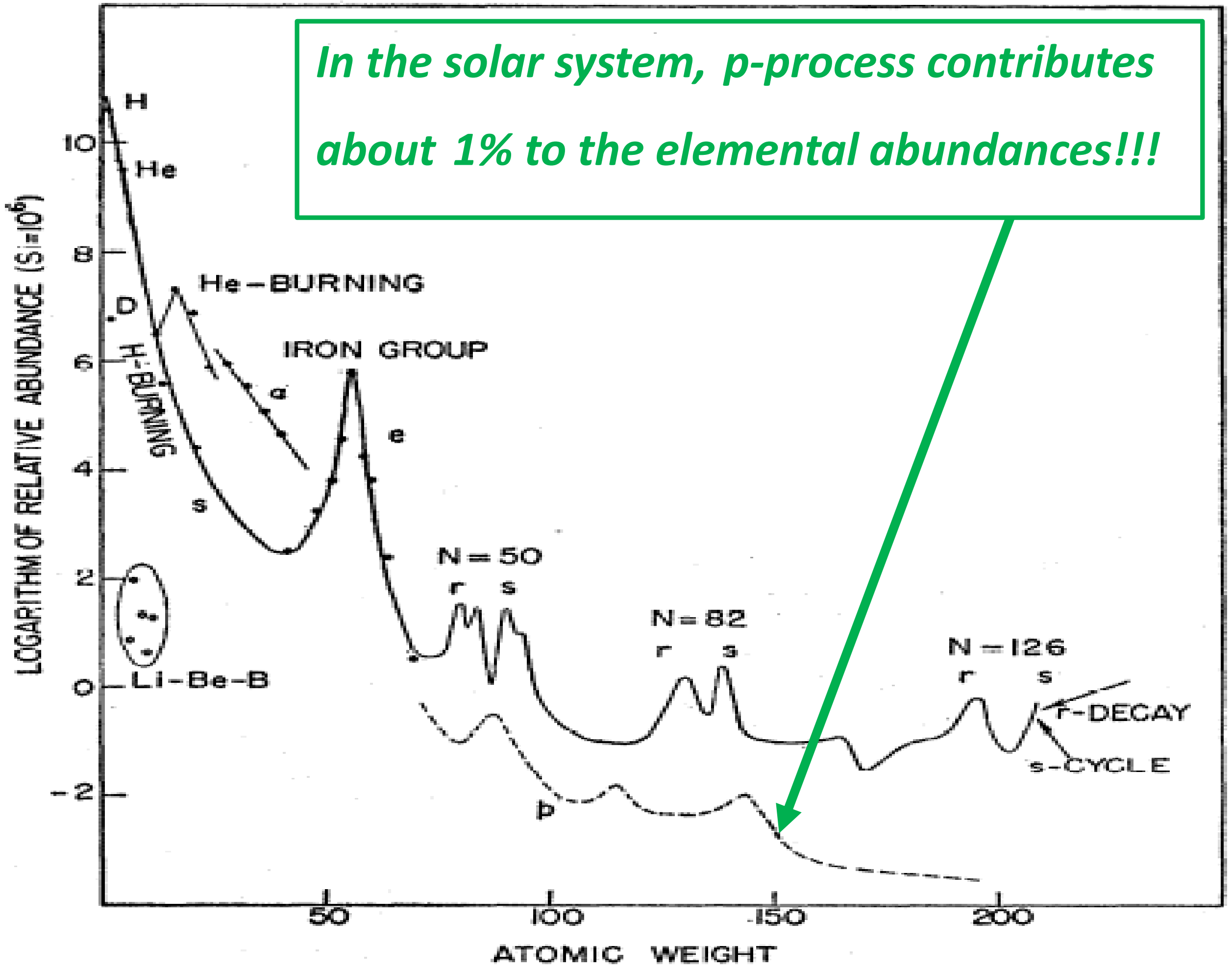

B²FH, Rev. Mod. Phys. 29, 547 (1957)

The *p*-process nucleosynthesis

- $\tau \sim 1s$ & $T \sim 2\text{-}3\ 10^9$K
- Photodisintegrations (γ,n), (γ,p), (γ,α)
- SNII (O-Ne & νp-wind) & SNIa

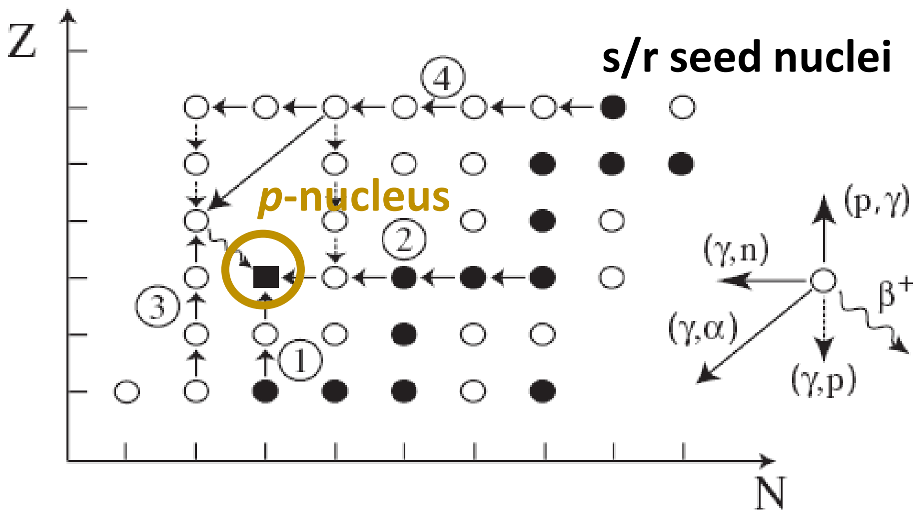

M. Arnould & S. Goriely, Phys. Rep. 384, 1 (2003)

P-nuclides yields obtained by convolution over a spectrum of stellar masses (assuming an Initital Mass Function)

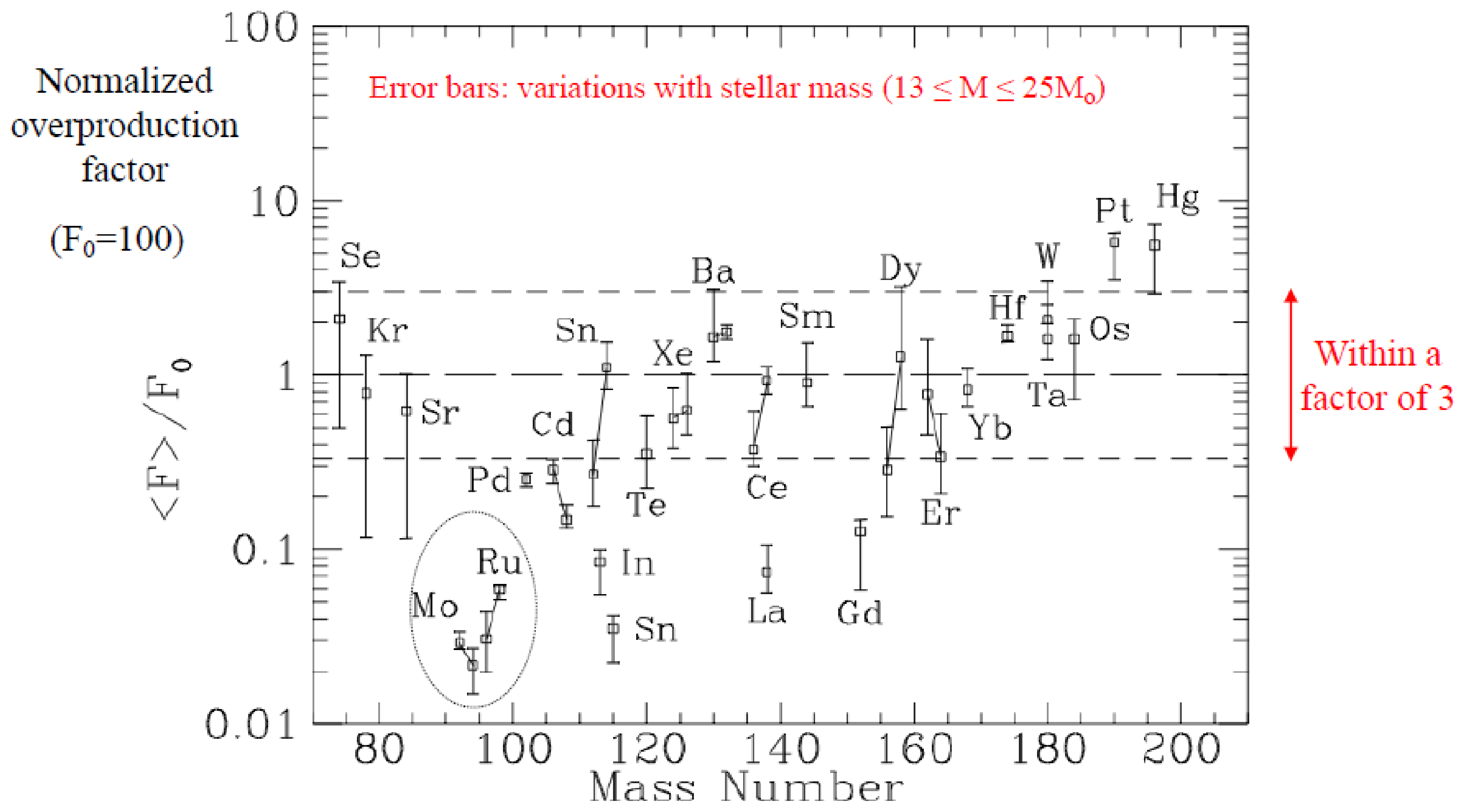

Some major discrepancies remain: Mo and Ru p-isotopes, ^{113}In, ^{115}Sn and ^{138}La.

Credits: S. Goriely

PHYSICAL REVIEW LETTERS

Accepted Paper

Production of p-nuclei from r-process seeds: The νr-process

Phys. Rev. Lett.

Zewei Xiong, Gabriel Martínez-Pinedo, Oliver Just, and Andre Sieverding

Accepted 13 March 2024

ABSTRACT

ABSTRACT

We present a nucleosynthesis process that may take place on neutron-rich ejecta experiencing an intensive neutrino flux. The nucleosynthesis proceeds similarly to the standard r-process, a sequence of neutron-captures and beta-decays, however with charged-current neutrino absorption reactions on nuclei operating much faster than beta-decays. Once neutron capture reactions freeze-out the produced r-process neutron-rich nuclei undergo a fast conversion of neutrons into protons and are pushed even beyond the β-stability line producing the neutron-deficient p-nuclei. This scenario, which we denote as the νr-process, provides an alternative channel for the production of p-nuclei and the short-lived nucleus ^{92}Nb. We discuss the necessary conditions posed on the astrophysical site for the νr-process to be realized in nature. While these conditions are not fulfilled by current neutrino-hydrodynamic models of r-process sites, future models, including more complex physics and a larger variety of outflow conditions, may achieve the necessary conditions in some regions of the ejecta.

***p*-Process Nucleosynthesis:**
an extended network of some 20000 reactions
linking about **2000 nuclei** in the A ≤ 210 mass range

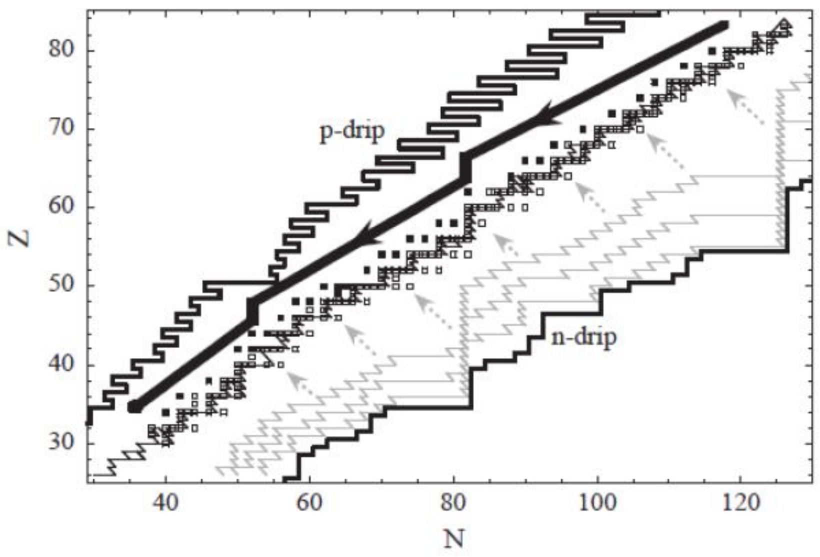

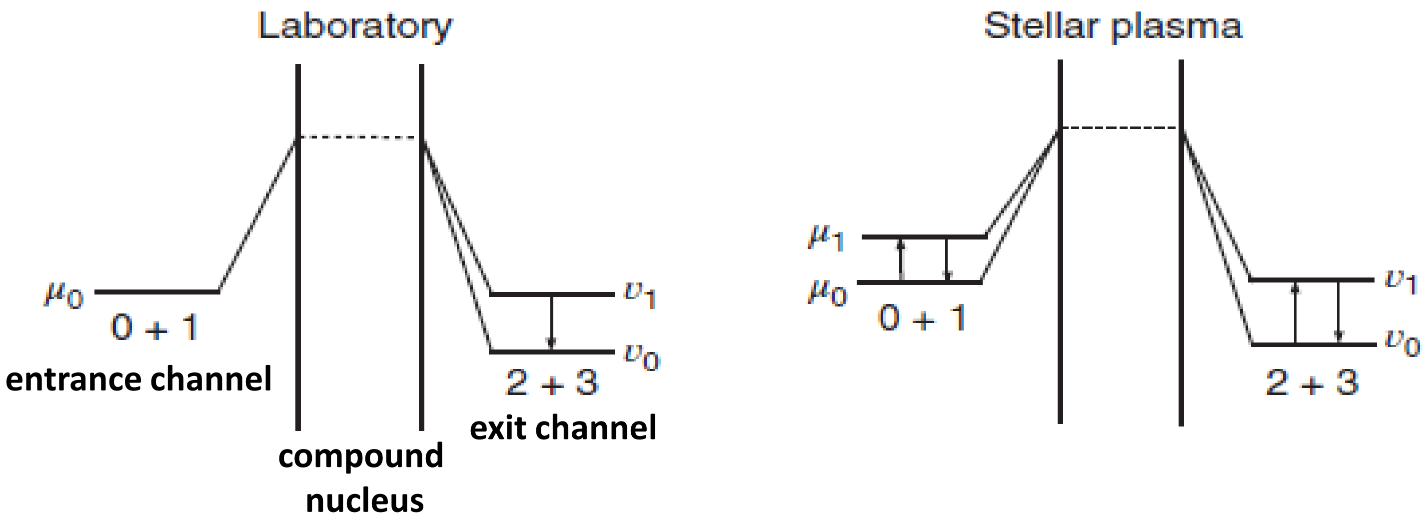

Image from C. Iliadis, Nuclear Physics of Stars (2007)

The **gs contribution** to the ***stellar rate*** for photodisintegration reactions concerning *p*-nuclei typically is only a few tenths per mille.

T. Rauscher, Ap. J. Suppl. 201, 26 (2012)

Photodisintegration experiments can only be used to derive information on certain nuclear properties required for the calculation of the stellar rates and, thus, to test and support the theory (statistical Hauser-Feshbach models)!!

- **Gamma-ray strength function**
- Nuclear level density
- Nucleon-nucleus optical potential

Photoneutron reaction cross section measurements on ^{94}Mo and ^{90}Zr relevant to the *p*-process nucleosynthesis

A. Banu* and E. G. Meekins†
Department of Physics and Astronomy, James Madison University, Harrisonburg, Virginia 22807, USA

J. A. Silano‡ and H. J. Karwowski
Triangle Universities Nuclear Laboratory, Durham, North Carolina 27708, USA and University of North Carolina at Chapel Hill, Chapel Hill, North Carolina 27516, USA

S. Goriely
Institut d'Astronomie et d'Astrophysique, Université Libre de Bruxelles, Campus de la Plaine, CP-226, 1050 Brussels, Belgium

(Received 10 June 2018; revised manuscript received 19 December 2018; published 11 February 2019)

The photodisintegration cross sections for the ^{94}Mo(γ, n) and ^{90}Zr(γ, n) reactions have been experimentally investigated with quasi-monochromatic photon beams at the High Intensity γ-ray Source (HIγS) facility of the Triangle Universities Nuclear Laboratory (TUNL). The energy dependence of the photoneutron reaction cross sections was measured with high precision from the respective neutron emission thresholds up to 13.5 MeV. These measurements contribute to a broader investigation of nuclear reactions relevant to the understanding of the *p*-process nucleosynthesis. The results are compared with the predictions of Hauser-Feshbach statistical model calculations using two different models for the dipole γ-ray strength function. The resulting ^{94}Mo(γ, n) and ^{90}Zr(γ, n) photoneutron stellar reaction rates as a function of temperature in the typical range of interest for the *p*-process nucleosynthesis show how sensitive the photoneutron stellar reaction rate can be to the experimental data in the vicinity of the neutron threshold.

Why study ^{94}Mo(γ,n)^{93}Mo & ^{90}Zr(γ,n)^{89}Zr?

- the most abundant *p*-nuclei, **^{92,94}Mo and ^{96,98}Ru**, are notoriously underproduced in the currently favored scenarios for the *p*-process, making their nucleosynthesis *a longstanding mystery in nuclear astrophysics*

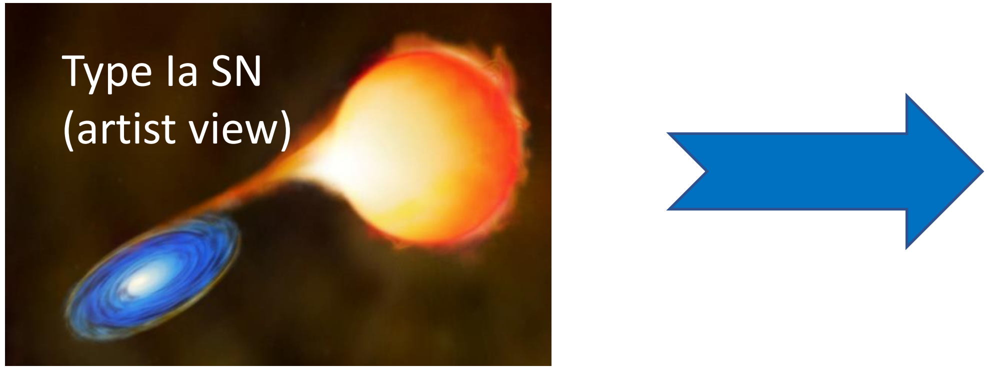

C. Travaglio et al., ApJ 739, 93 (2011);
C. Travaglio et al., ApJ 799, 54 (2015)

- ✓ *"For the first time, we find a stellar source able to produce both light and heavy p-nuclei almost at the same level as ^{56}Fe, including the debated ^{92,94}Mo and ^{96,98}Ru."*
- ✓ *"[...], we estimate that SNe Ia can contribute to at least 50% of the solar p-process composition."*

❖ Enhanced *s*-process seed distributions assumed!!!

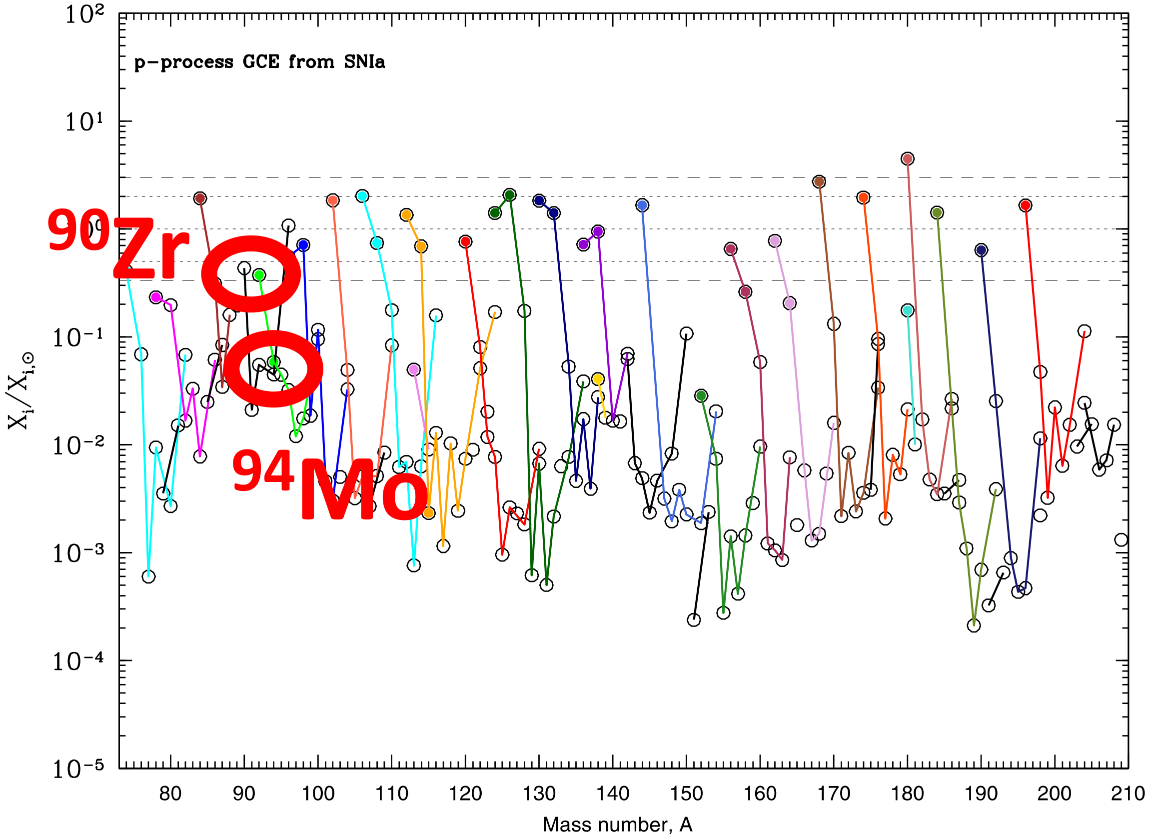

- (only!) **^{94}Mo** underproduced
- An important contribution from the *p*-process nucleosynthesis to the neutron magic nucleus **^{90}Zr** (a genuine *s*-process nucleus)

High Intensity Gamma-ray Source (HIGS) at TUNL

- Highest intensity (γ-rays/s/keV) γ-ray beam in the world
- Produces γ-rays by Compton backscattering inside the optical cavity of a storage-ring FEL
- Produces both linearly and circularly polarized beams

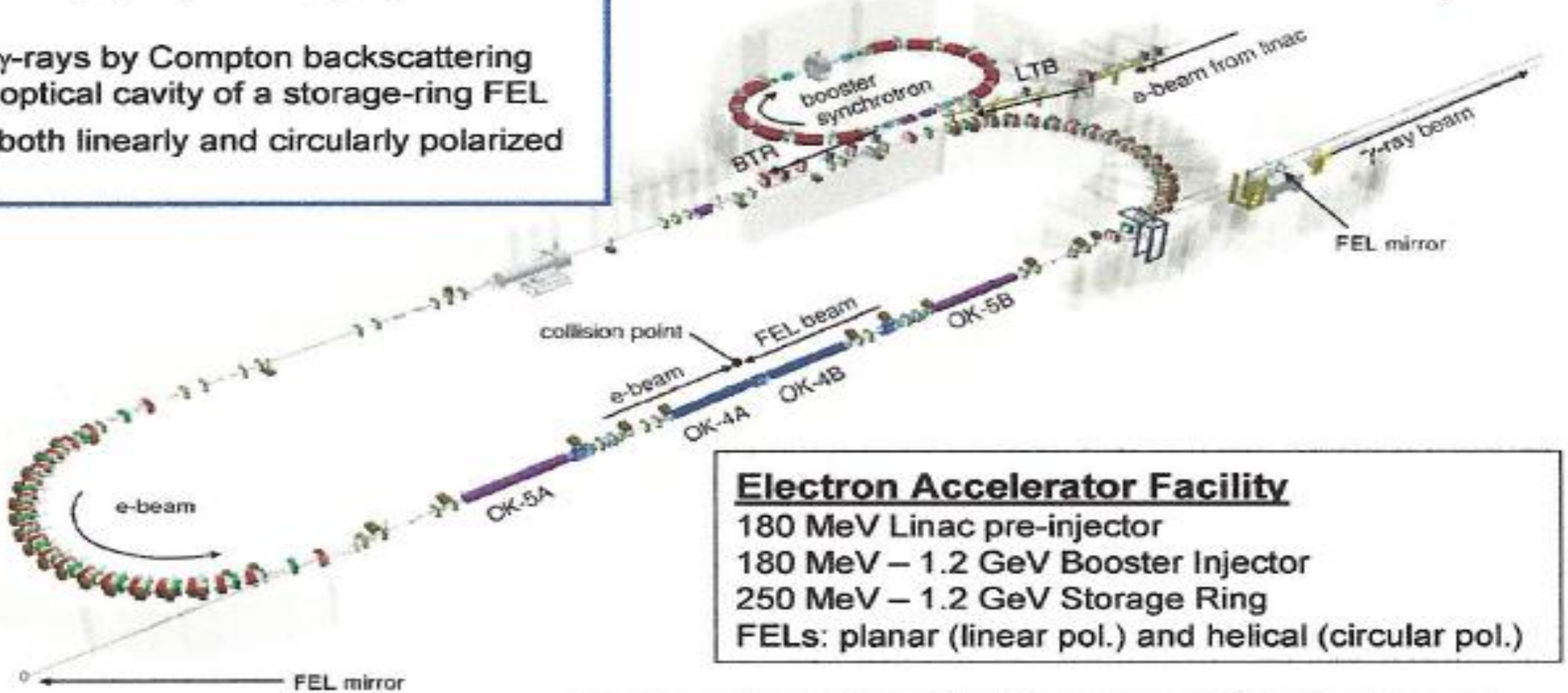

Electron Accelerator Facility
180 MeV Linac pre-injector
180 MeV – 1.2 GeV Booster Injector
250 MeV – 1.2 GeV Storage Ring
FELs: planar (linear pol.) and helical (circular pol.)

γ-ray beam parameters	Values
Energy	1 – 100 MeV
Linear & circular polarization	> 95%
Intensity with 5% $\Delta E_\gamma/E_\gamma$	> 10^7 γ/s

For more details see:
http://www.tunl.duke.edu/higs/

How HIγS Works: Laser Compton Backscattering (LCB)

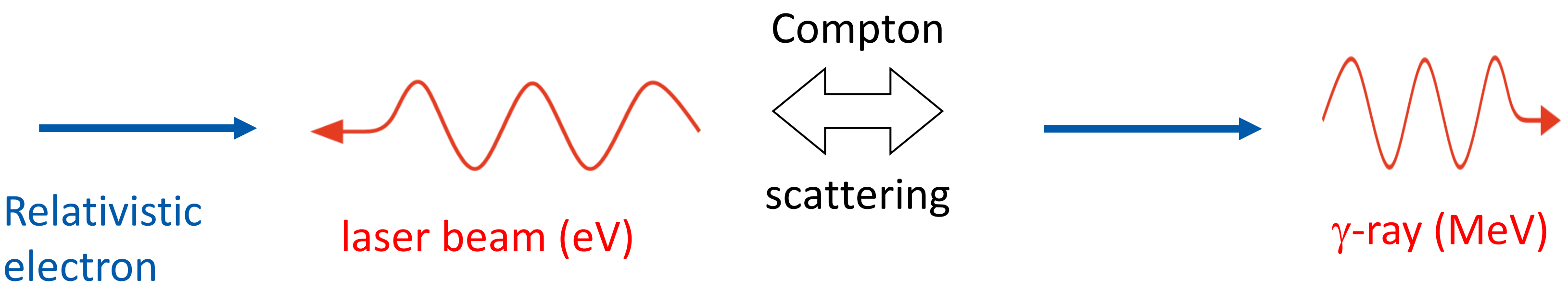

$$E_\gamma = \frac{\hbar\omega \cdot (1-\beta\cdot\cos\theta_i)}{1-\beta\cdot\cos\theta_f + \frac{\hbar\omega}{E_{electron}}(1-\cos\theta_{photon})} \approx 4\gamma^2 \cdot E_{laser}$$

$\gamma = E_e/mc^2$ (Lorentz factor)

Example:

E_{laser} = 3.3 eV

$E_{electron}$ = 450 MeV (γ = 882)

E_γ = 10 MeV

LCB facilities in the world:

- HIγS @ TUNL/Duke University (USA)
- ~~NewSUBARU~~ (Japan); BL01 γ- ray beam usage ended on March 31, 2021
- VEGA @ ELI-NP (Romania); under implementation (*estimated to become available in 2026*)

Experimental Setup

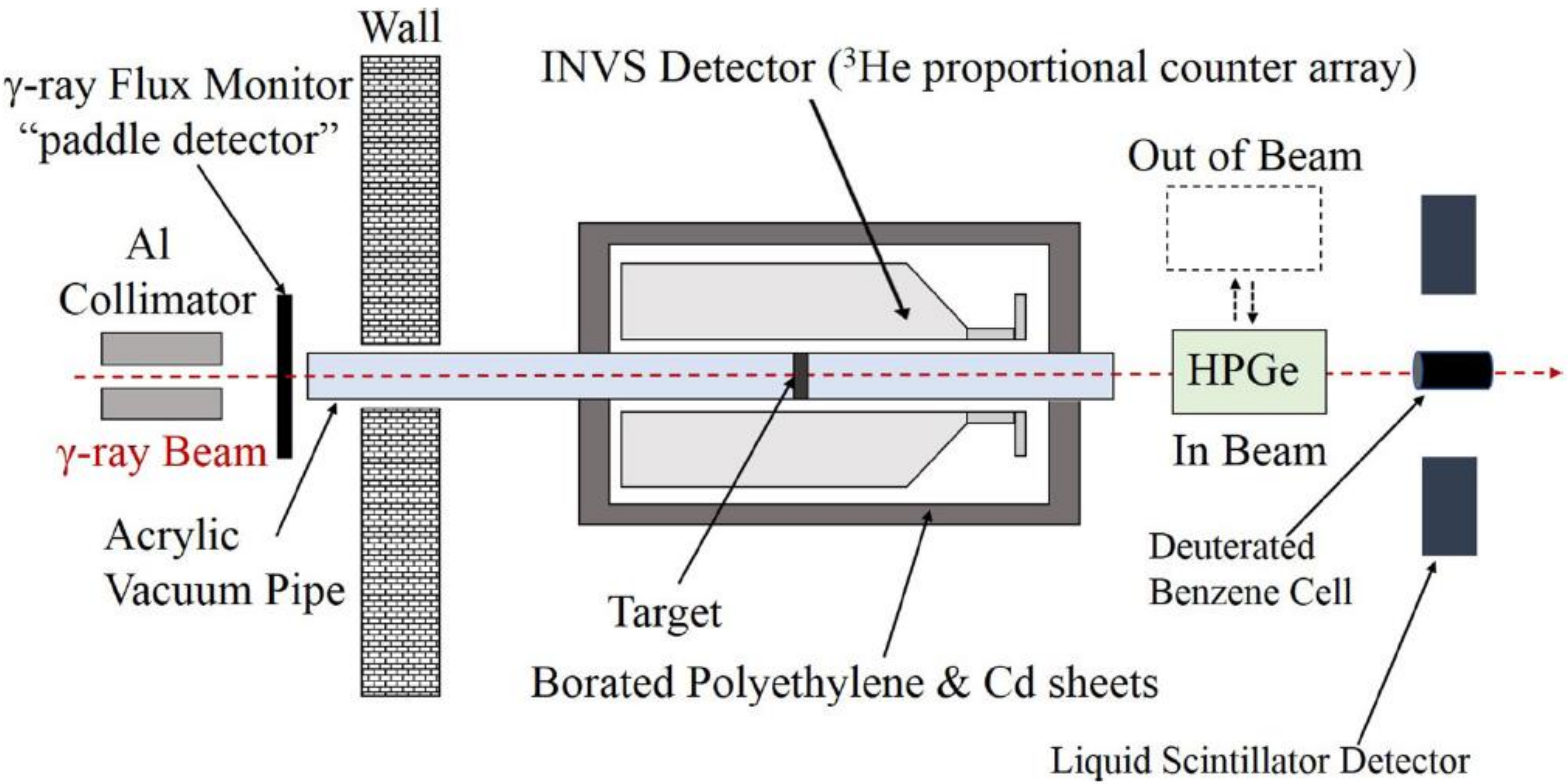

~ $10^7 – 10^8$ γ/s

✧ ^{94}Mo: ~ 600 mg/cm^2, 98.97%
✧ ^{90}Zr: ~ 1 g/cm^2, 97.7%

$\Delta E_\gamma / E_\gamma \sim 4\% - 5\%$

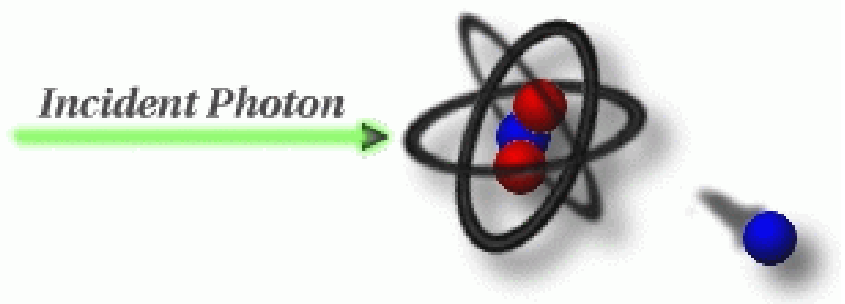

$$\gamma + {}^{90}Zr \rightarrow {}^{90}Zr^{*} \rightarrow {}^{89}Zr + n$$

γ-ray Beam Energies (MeV):

12, 12.1, 12.2, 12.4, 12.5, 12.8, 13, 13.5

(only g.s. neutrons) (g.s./excited-state neutrons)

$$\sigma(E_\gamma) = \frac{N_n}{N_\gamma N_t \varepsilon_n(E_\gamma)}$$

N_n – number of neutrons detected using ^{3}He counters

N_γ - number of incident photons

N_t – number of target atoms per unit area (enriched target)

ε_n – neutron detection efficiency

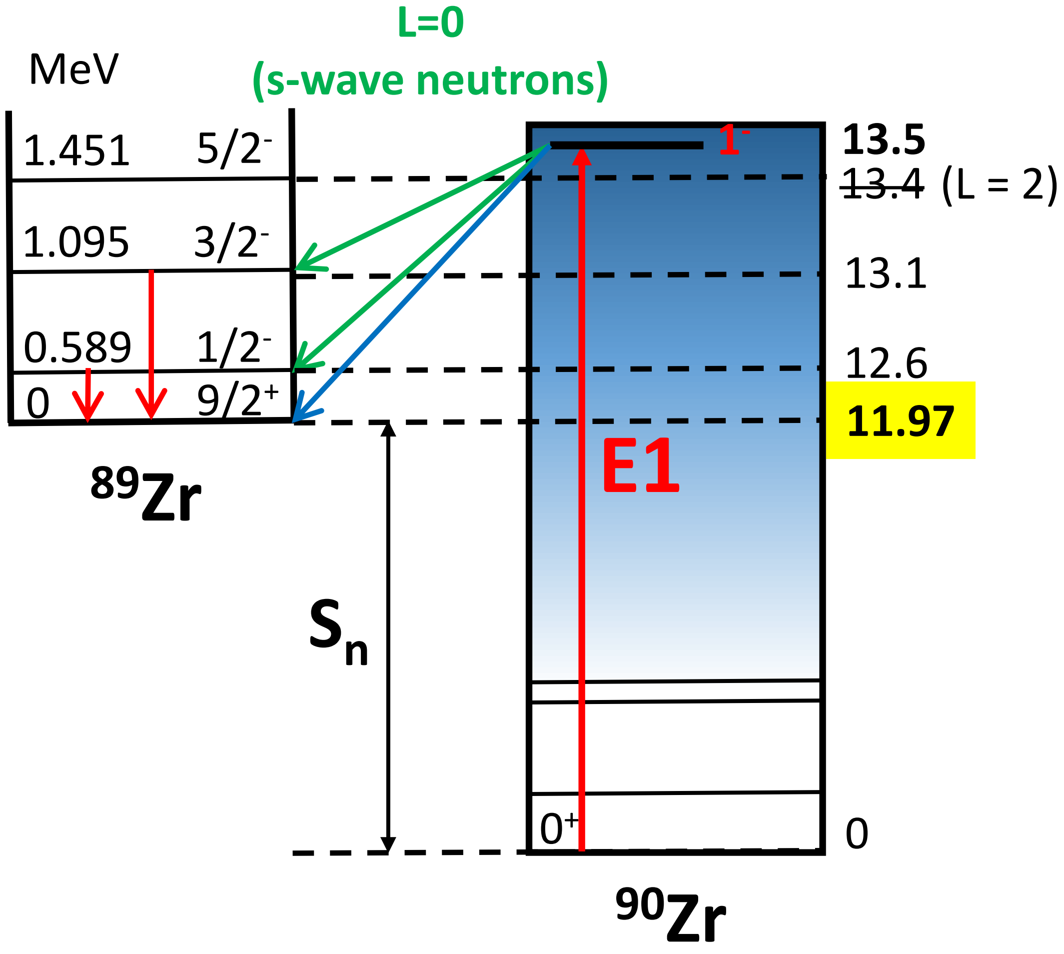

Neutron Detection Efficiency

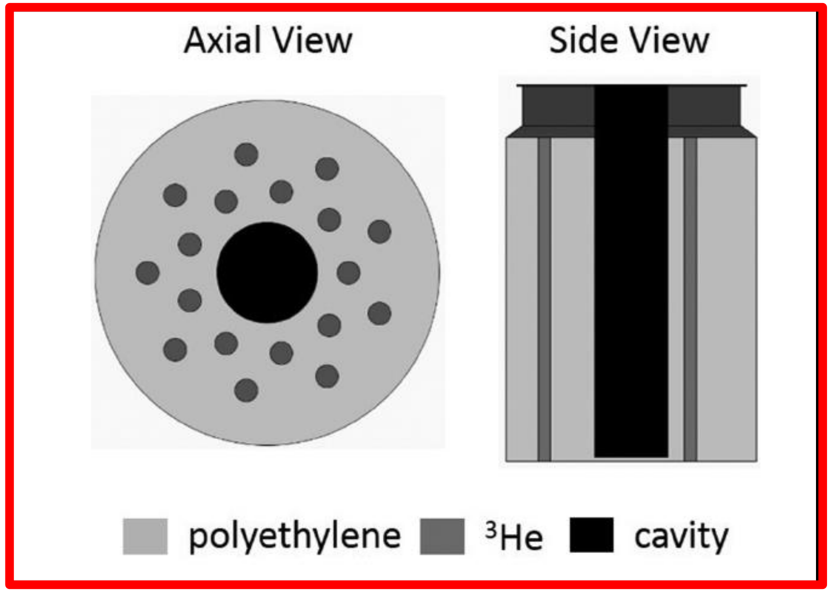

C. W. Arnold et al., Nucl. Instr. and Meth. A 647, 55 (2011)

Neutron energy is lost by the **thermalization** of neutrons in the moderator (polyethylene)!!

- Simulated efficiencies for neutron energies of interest:

~55% @ 20 keV - ~25% @ 4 MeV

$$E_{n0} = \left(\frac{A-1}{A}\right)(E_\gamma - S_n)$$ (for g.s. neutrons)

$$E_{ni} = \left(\frac{A-1}{A}\right)(E_\gamma - S_n - E_i)$$ (for excited-state neutrons)

$\varepsilon_{ni}(E_{ni})$ – neutron efficiency from Geant4 simulations

b_i – neutron branching from TALYS calculations

Effective neutron efficiency:

$$\epsilon_n^{\mathrm{eff}} = \sum_i b_i \epsilon_{n_i}(E_{n_i})$$

$^{90}Zr(\gamma,n)^{89}Zr$

E_γ (MeV)	E_i (MeV)	$J_i^{\pi_i}$	E_{n_i} (MeV)	l_i	ϵ_{n_i} (%)	b_i	$\epsilon_n^{\mathrm{eff}}$ (%)
12	0	$9/2^+$	0.03	3 (*f* wave)	52.89	1	**52.89**
12.1	0	$9/2^+$	0.13	3 (*f* wave)	52.15	1	**52.15**
12.2	0	$9/2^+$	0.23	3 (*f* wave)	51.53	1	**51.53**
12.4	0	$9/2^+$	0.43	3 (*f* wave)	49.21	1	**49.21**
12.5	0	$9/2^+$	0.53	3 (*f* wave)	47.69	1	**47.69**
12.8	0	$9/2^+$	0.82	3 (*f* wave)	44.18	0.17	**49.94**
	0.5878	$1/2^-$	0.24	0 (*s* wave)	51.12	0.83	
13	0	$9/2^+$	1.02	3 (*f* wave)	41.33	0.23	**46.94**
	0.5878	$1/2^-$	0.44	0 (*s* wave)	48.61	0.77	
13.5	0	$9/2^+$	1.51	3 (*f* wave)	36.71	0.26	**42.97**
	0.5878	$1/2^-$	0.93	0 (*s* wave)	42.68	0.45	
	1.0949	$3/2^-$	0.43	0 (*s* wave)	49.02	0.29	

$^{90}Zr(\gamma,n)^{89}Zr$

E_γ (MeV)	σ_{E_γ} (MeV)	$\sigma_{(\gamma,n)}$ (mb)	$\eta = \frac{\epsilon_{n0}}{\epsilon_n^{eff}} = \frac{\sigma_{(\gamma,n)}}{\sigma_{(\gamma,n_0)}}$	
11.75	0.21	0.01 ± 0.01	1	
12	0.23	0.11 ± 0.01	1	
12.1	0.21	0.14 ± 0.02	1	
12.2	0.22	0.50 ± 0.03	1	
12.4	0.22	2.28 ± 0.12	1	
12.5	0.23	4.42 ± 0.24	1	
12.8	0.23	9.67 ± 0.52	0.88	1 excited state
13	0.22	12.66 ± 0.68	0.88	1 excited state
13.5	0.24	20.94 ± 1.13	0.85	2 excited states

$^{90}Zr(\gamma,n)^{89}Zr$

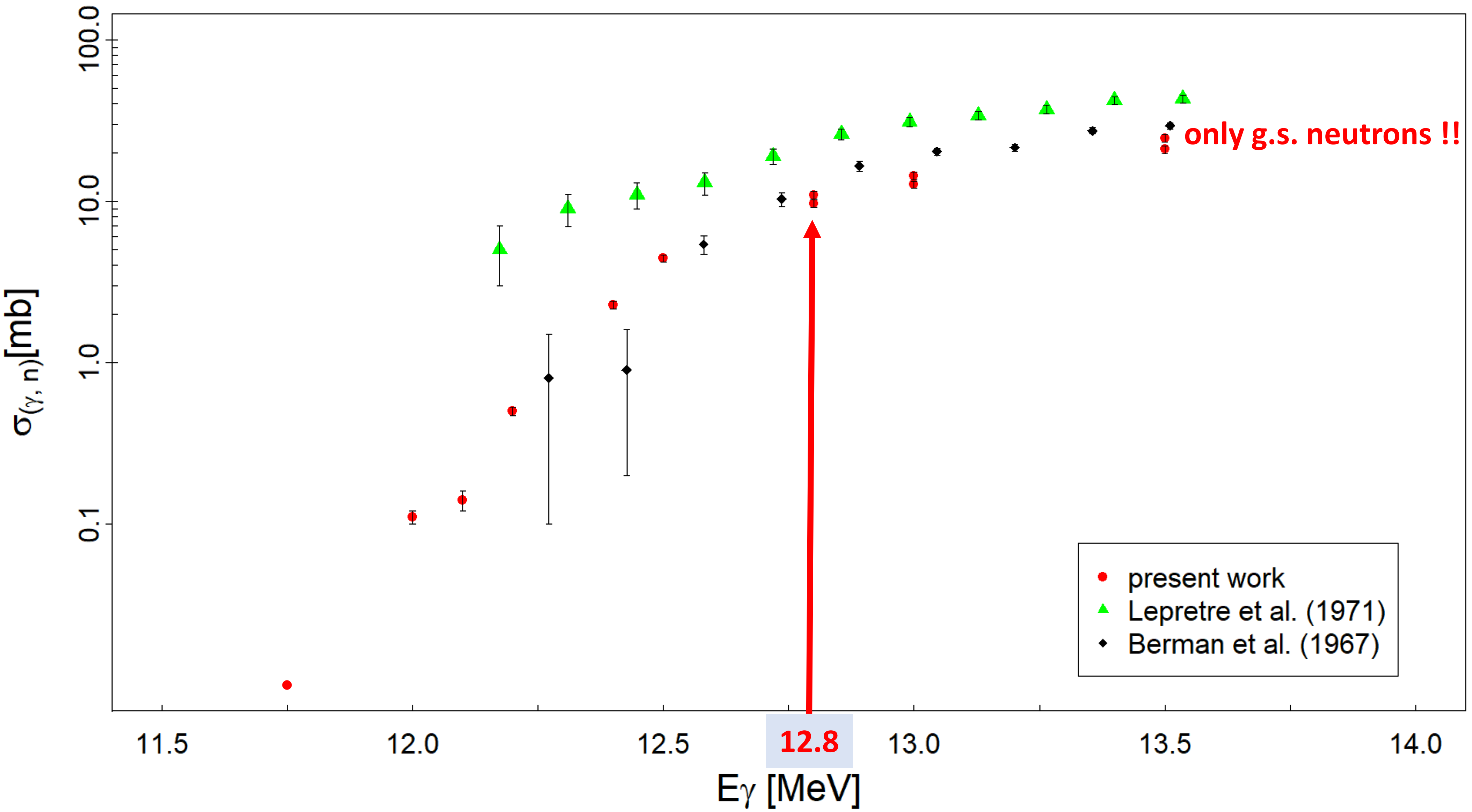

$^{94}Mo(\gamma,n)^{93}Mo$

E_γ (MeV)	σ_{E_γ} (MeV)	$\sigma_{(\gamma,n)}$ (mb)	$\eta = \frac{\epsilon_{n0}}{\epsilon_n^{eff}} = \frac{\sigma_{(\gamma,n)}}{\sigma_{(\gamma,n_0)}}$	
9.5	0.18	0.28 ± 0.02	1	
9.6	0.17	1.21 ± 0.07	1	
9.65	0.17	2.51 ± 0.14	1	
9.7	0.17	2.97 ± 0.16	1	
9.75	0.17	4.50 ± 0.24	1	
9.8	0.17	4.93 ± 0.27	1	
9.85	0.17	6.28 ± 0.34	1	
9.95	0.16	7.83 ± 0.42	1	
10	0.19	8.44 ± 0.46	1	
10.2	0.17	10.11 ± 0.55	1	
10.5	0.17	11.77 ± 0.63	1	
10.8	0.17	13.06 ± 0.70	0.89	1 excited state
11	0.17	14.53 ± 0.78	0.86	1 excited state
11.5	0.24	17.47 ± 0.94	0.80	3 excited states
11.65	0.25	18.73 ± 1.01	0.78	3 excited states
11.8	0.22	20.63 ± 1.11	0.79	3 excited states
11.95	0.23	22.61 ± 1.22	0.79	6 excited states
12.25	0.22	24.20 ± 1.30	0.71	8 excited states
12.5	0.23	27.86 ± 1.50	0.72	11 excited states
12.8	0.23	32.39 ± 1.74	0.74	14 excited states
13.5	0.24	48.64 ± 2.62	0.77	22 excited states

E_γ (MeV)	E_i (MeV)	$J_i^{\pi_i}$	E_{n_i} (MeV)	l_i	ϵ_{n_i} (%)	b_i	$\epsilon_n^{\mathrm{eff}}$ (%)
9.7	0	$5/2^+$	0.02	1 (p wave)	53.79	1	**53.79**
9.75	0	$5/2^+$	0.07	1 (p wave)	53.29	1	**53.29**
9.8	0	$5/2^+$	0.12	1 (p wave)	53.03	1	**53.03**
9.85	0	$5/2^+$	0.17	1 (p wave)	52.44	1	**52.44**
9.95	0	$5/2^+$	0.27	1 (p wave)	51.45	1	**51.45**
10	0	$5/2^+$	0.32	1 (p wave)	50.30	1	**50.30**
10.2	0	$5/2^+$	0.52	1 (p wave)	47.74	1	**47.74**
10.5	0	$5/2^+$	0.81	1 (p wave)	44.03	1	**44.03**
10.8	0	$5/2^+$	1.11	1 (p wave)	40.51	0.59	**45.35**
	0.9433	$1/2^+$	0.18	1 (p wave)	52.32	0.41	
11	0	$5/2^+$	1.31	1 (p wave)	38.37	0.46	**44.73**
	0.9433	$1/2^+$	0.37	1 (p wave)	50.15	0.54	
11.5	0	$5/2^+$	1.80	1 (p wave)	34.35	0.31	**42.83**
	0.9433	$1/2^+$	0.87	1 (p wave)	43.23	0.37	
	1.4925	$3/2^+$	0.33	1 (p wave)	50.19	0.26	
	1.6950	$5/2^+$	0.13	1 (p wave)	52.18	0.06	
11.65	0	$5/2^+$	1.95	1 (p wave)	33.14	0.29	**42.46**
	0.9433	$1/2^+$	1.02	1 (p wave)	41.68	0.33	
	1.4925	$3/2^+$	0.47	1 (p wave)	48.39	0.28	
	1.6950	$5/2^+$	0.27	1 (p wave)	50.43	0.10	
11.8	0	$5/2^+$	2.10	1 (p wave)	32.25	0.29	**40.71**
	0.9433	$1/2^+$	1.17	1 (p wave)	39.94	0.30	
	1.4925	$3/2^+$	0.62	1 (p wave)	46.42	0.28	
	1.6950	$5/2^+$	0.42	1 (p wave)	49.04	0.13	
11.95	0	$5/2^+$	2.25	1 (p wave)	32.99	0.26	**41.57**
	0.9433	$1/2^+$	1.31	1 (p wave)	38.36	0.25	
	1.4925	$3/2^+$	0.77	1 (p wave)	44.66	0.24	
	1.6950	$5/2^+$	0.57	1 (p wave)	47.25	0.11	
	2.1420	$5/2^+$	0.129	1 (p wave)	52.30	0.04	
	2.1454	$3/2^+, 5/2^+$	0.125	1 (p wave)	52.32	0.07	
	2.1811	$3/2^+$	0.09	1 (p wave)	52.83	0.03	
12.25	0	$5/2^+$	2.25	1 (p wave)	29.54	0.23	**41.32**
	0.9433	$1/2^+$	1.61	1 (p wave)	35.57	0.16	
	1.4925	$3/2^+$	1.07	1 (p wave)	40.99	0.17	
	1.6950	$5/2^+$	0.87	1 (p wave)	43.44	0.08	
	2.1420	$5/2^+$	0.43	1 (p wave)	48.93	0.07	
	2.1454	$3/2^+, 5/2^+$	0.42	1 (p wave)	48.92	0.12	
	2.1811	$3/2^+$	0.39	1 (p wave)	49.72	0.12	
	2.4374	$1/2^+$	0.13	1 (p wave)	51.98	0.04	
	2.5297	$1/2^-, 3/2^-$	0.04	0 (s wave)	52.82	0.01	

$^{94}Mo(\gamma,n)^{93}Mo$

$^{94}Mo(\gamma,n)^{93}Mo$

E_γ (MeV)	E_i (MeV)	$J_i^{\pi_i}$	E_{n_i} (MeV)	l_i	ϵ_{n_i} (%)	b_i	$\epsilon_n^{\rm eff}$ (%)
12.5	0	$5/2^+$	2.79	1 (*p* wave)	28.78	0.23	**39.86**
	0.9433	$1/2^+$	1.86	1 (*p* wave)	33.87	0.10	
	1.4925	$3/2^+$	1.32	1 (*p* wave)	38.37	0.19	
	1.6950	$5/2^+$	1.12	1 (*p* wave)	40.45	0.06	
	2.1420	$5/2^+$	0.673	1 (*p* wave)	45.74	0.05	
	2.1454	$3/2^+, 5/2^+$	0.669	1 (*p* wave)	45.60	0.10	
	2.1811	$3/2^+$	0.63	1 (*p* wave)	46.26	0.10	
	2.4374	$1/2^+$	0.38	1 (*p* wave)	49.81	0.08	
	2.5297	$1/2^-, 3/2^-$	0.29	0 (*s* wave)	50.60	0.01	
	2.6190	$1/2^-, 3/2^-$	0.20	0 (*s* wave)	51.55	0.01	
	2.6701	$1/2^+$	0.15	1 (*p* wave)	52.15	0.04	
	2.7046	$1/2^+$	0.12	1 (*p* wave)	52.26	0.03	
12.8	0	$5/2^+$	3.09	1 (*p* wave)	27.66	0.28440	**37.16**
	0.9433	$1/2^+$	2.16	1 (*p* wave)	31.84	0.07408	
	1.4925	$3/2^+$	1.61	1 (*p* wave)	35.74	0.14420	
	1.6950	$5/2^+$	1.41	1 (*p* wave)	37.65	0.07771	
	2.1420	$5/2^+$	0.970	1 (*p* wave)	42.27	0.03704	
	2.1454	$3/2^+, 5/2^+$	0.966	1 (*p* wave)	42.25	0.07167	
	2.1811	$3/2^+$	0.93	1 (*p* wave)	46.46	0.06981	
	2.4374	$1/2^+$	0.68	1 (*p* wave)	45.92	0.06373	
	2.5297	$1/2^-, 3/2^-$	0.59	0 (*s* wave)	46.71	0.01074	
	2.6190	$1/2^-, 3/2^-$	0.50	0 (*s* wave)	48.01	0.00883	
	2.6701	$1/2^+$	0.45	1 (*p* wave)	48.90	0.05549	
	2.7046	$1/2^+$	0.41	1 (*p* wave)	49.35	0.05335	
	2.8421	$1/2^+$	0.28	1 (*p* wave)	50.66	0.04113	
	2.9552	$1/2^-, 3/2^-$	0.17	0 (*s* wave)	51.80	0.00499	
	3.0640	$1/2^-, 3/2^-$	0.06	0 (*s* wave)	52.66	0.00283	
13.5	0	$5/2^+$	3.78	1 (*p* wave)	25.35	0.32964	**32.93**
	0.9433	$1/2^+$	2.85	1 (*p* wave)	28.48	0.07525	
	1.4925	$3/2^+$	2.30	1 (*p* wave)	30.79	0.10762	
	1.6950	$5/2^+$	2.10	1 (*p* wave)	32.17	0.07133	
	2.1420	$5/2^+$	1.660	1 (*p* wave)	35.24	0.03091	
	2.1454	$3/2^+, 5/2^+$	1.659	1 (*p* wave)	35.27	0.05072	
	2.1811	$3/2^+$	1.62	1 (*p* wave)	35.53	0.04801	
	2.4374	$1/2^+$	1.37	1 (*p* wave)	38.07	0.04383	
	2.5297	$1/2^-, 3/2^-$	1.28	0 (*s* wave)	38.71	0.01244	
	2.6190	$1/2^-, 3/2^-$	1.19	0 (*s* wave)	39.69	0.00935	
	2.6701	$1/2^+$	1.14	1 (*p* wave)	40.15	0.04146	
	2.7046	$1/2^+$	1.11	1 (*p* wave)	40.43	0.04142	
	2.8421	$1/2^+$	0.97	1 (*p* wave)	42.03	0.04114	
	2.9552	$1/2^-, 3/2^-$	0.86	0 (*s* wave)	43.52	0.00869	
	3.0640	$1/2^-, 3/2^-$	0.75	0 (*s* wave)	44.92	0.00680	
	3.1592	$3/2^+, 5/2^+$	0.66	1 (*p* wave)	45.77	0.02017	
	3.3876	$3/2^+, 5/2^+$	0.43	1 (*p* wave)	48.92	0.01743	
	3.4503	$3/2^+, 5/2^+$	0.37	1 (*p* wave)	49.78	0.03078	
	3.5900	$1/2^-, 3/2^-$	0.23	0 (*s* wave)	50.66	0.00354	
	3.5963	$3/2^+, 5/2^+$	0.22	1 (*p* wave)	51.08	0.00348	
	3.7089	$3/2^+, 5/2^+$	0.11	1 (*p* wave)	52.06	0.00241	
	3.7200	$1/2^-, 3/2^-$	0.10	0 (*s* wave)	52.33	0.00229	
	3.7900	$1/2^-, 3/2^-$	0.03	0 (*s* wave)	52.57	0.00129	

$^{94}Mo(\gamma,n)^{93}Mo$

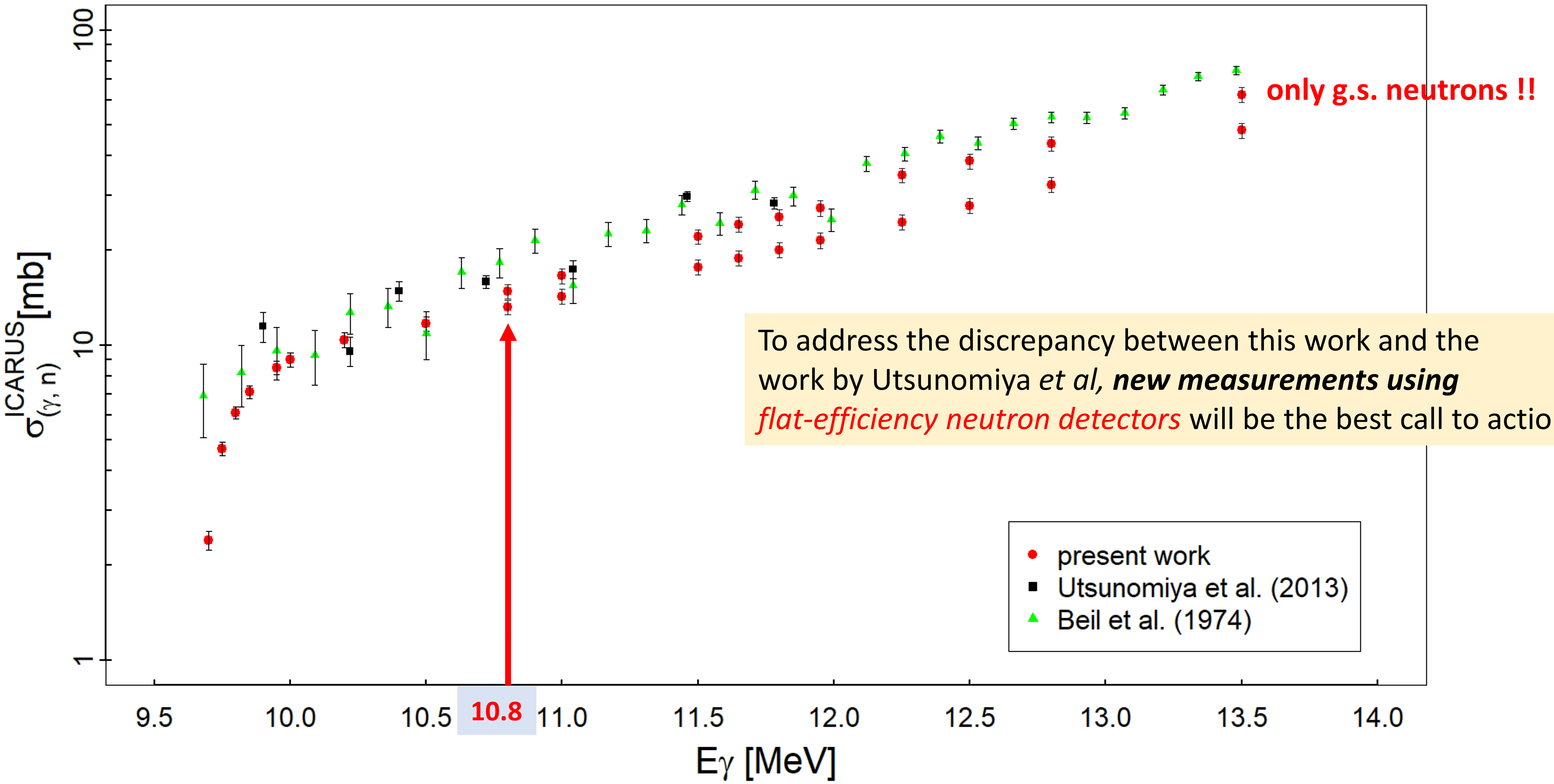

To address the discrepancy between this work and the work by Utsunomiya *et al*, ***new measurements using*** *flat-efficiency neutron detectors* will be the best call to action!

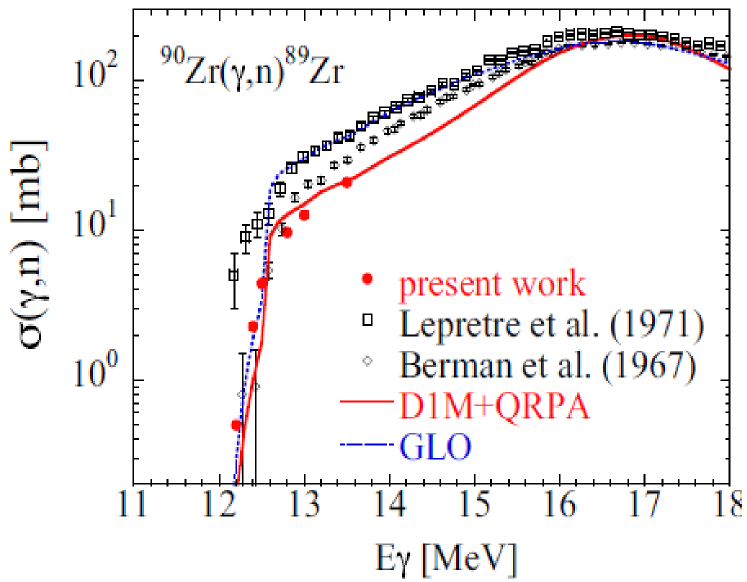

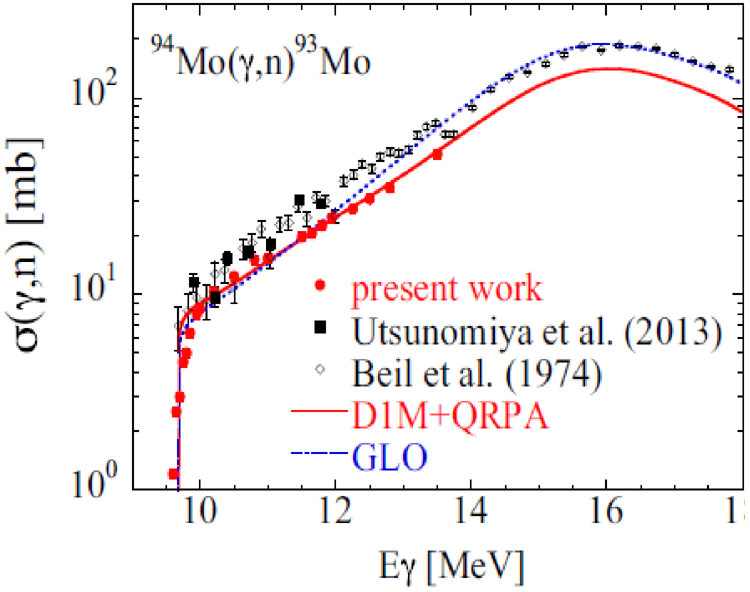

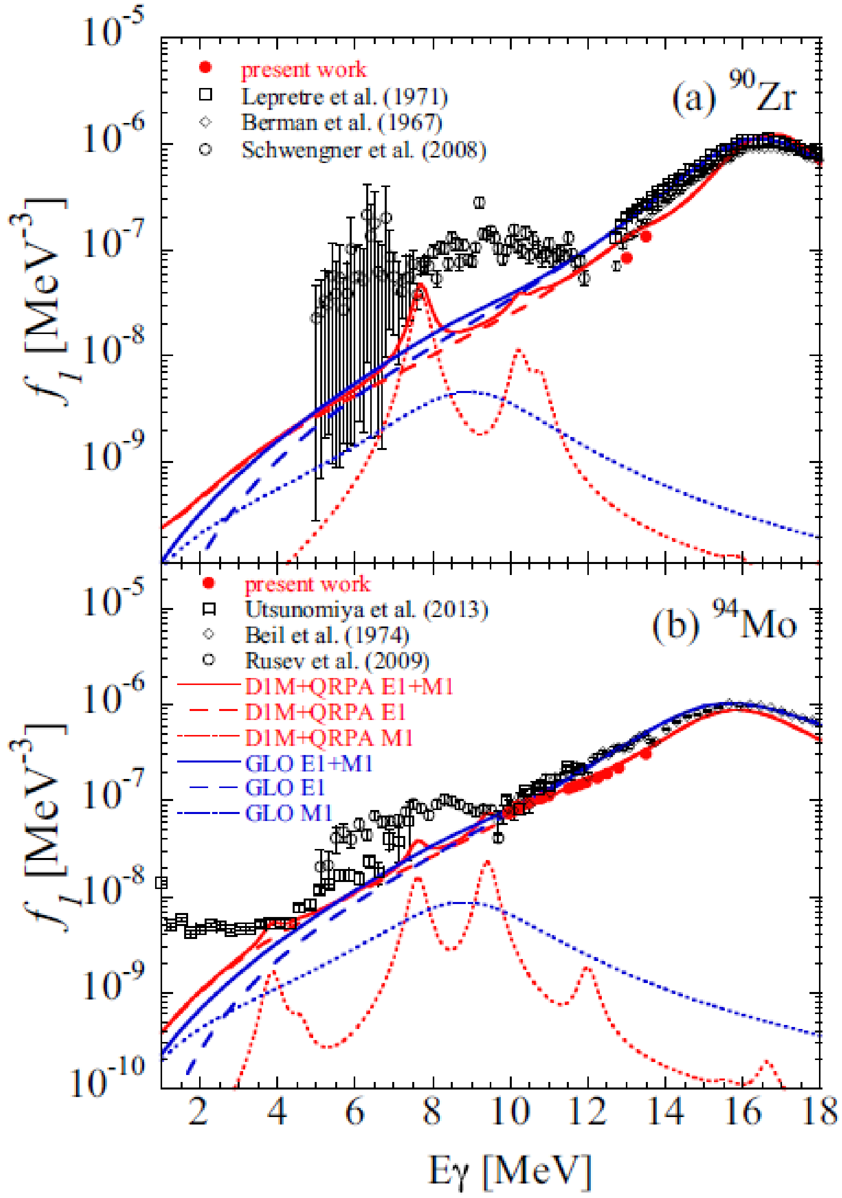

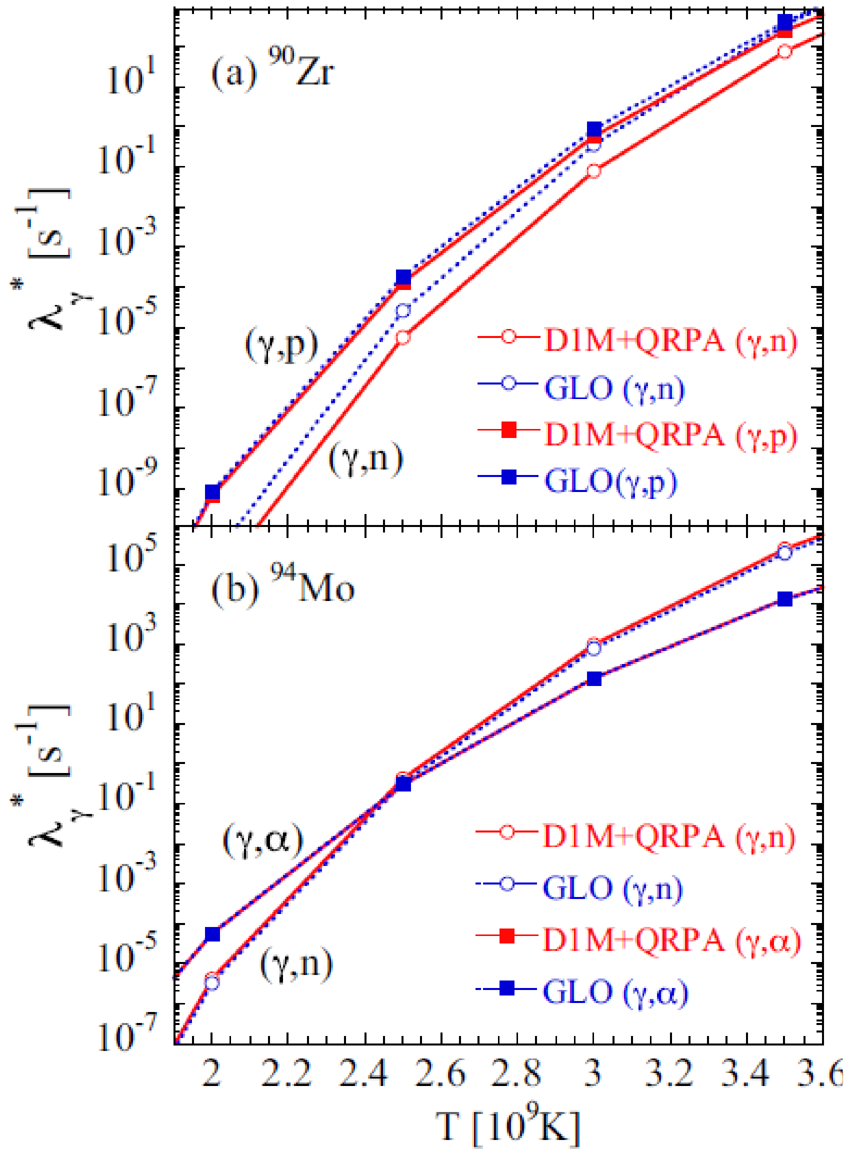

$$f(E_\gamma) = \frac{1}{3\pi^2\hbar^2c^2}\frac{\sigma_\gamma(E_\gamma)}{E_\gamma}$$

A. Banu *et al.*, Phys. Rev. C 99, 025802 (2019)

Nuclear Resonance Fluorescence (NRF) Measurements on ^{78,80}Kr to determine the γSF for *p*-process nucleosynthesis calculations

No γSF data available for ^{78,80}Kr!!

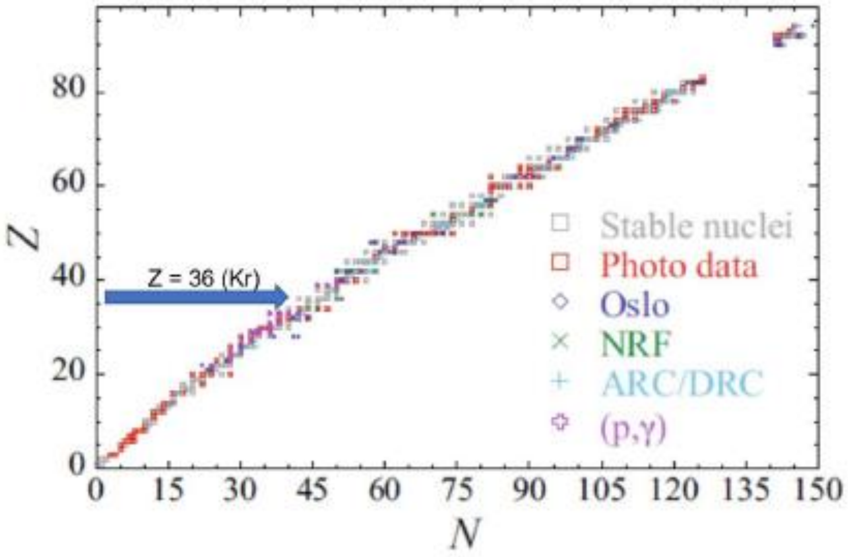

S. Goriely et al, Eur. Phys. J. A 55, 172 (2019)

PHYSICAL REVIEW C 73, 015804 (2006)

Branchings in the γ process path revisited

Thomas Rauscher*
Departement für Physik und Astronomie, Universität Basel, CH-4056 Basel, Switzerland

TABLE II. Nuclei with large rate uncertainties (derived from rate set **A** [10], see text); subscripts at each neutron number indicate which rate ($\lambda_{\gamma p}$ or $\lambda_{\gamma\alpha}$) is close to the $\lambda_{\gamma n}$ rate within factors of 3 and 10, respectively.

Z	Neutron number N at given temperature T_9		
	2.0	2.5	3.0
34	42_α		
35	46_p	46_p	
36	$44_{p,\alpha}$	44_p	
37		48_p	45_p, 48_p
38	43_p	43_p, 46_p	46_p
39	49_p	49_p	49_p
40	47_p	50_p	50_p

^{80}Kr was identified as *a key branching point*, for which the (γ,p) and (γ,α) reaction rates were found to be larger than the (γ,n) rate – NON-SMOKER calculations with GLO model for γSF & a shifted Fermi-gas model for NLD.

TALYS calculations with the **D1M+QRPA γSF model** and HFB plus combinatorial NLD model

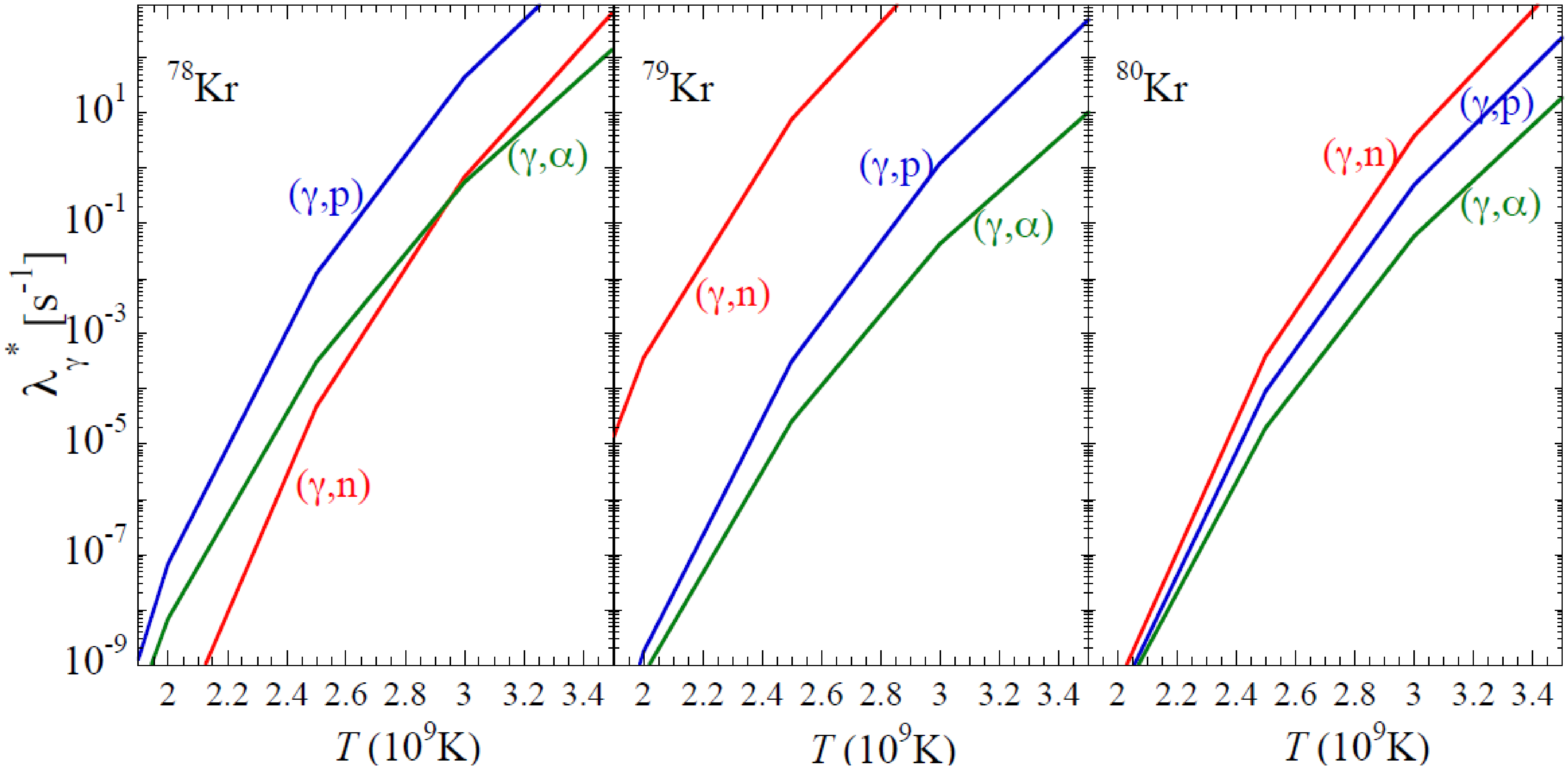

Contrary to NON-SMOKER calculations, TALYS calculations indicate the dominance of the ^{80}Kr(γ,n) channel over the ^{80}Kr(γ,p) and ^{80}Kr(γ,α) channels => **^{78}Kr production follows the path ^{80}Kr(γ,n)^{79}Kr(γ,n)^{78}Kr**

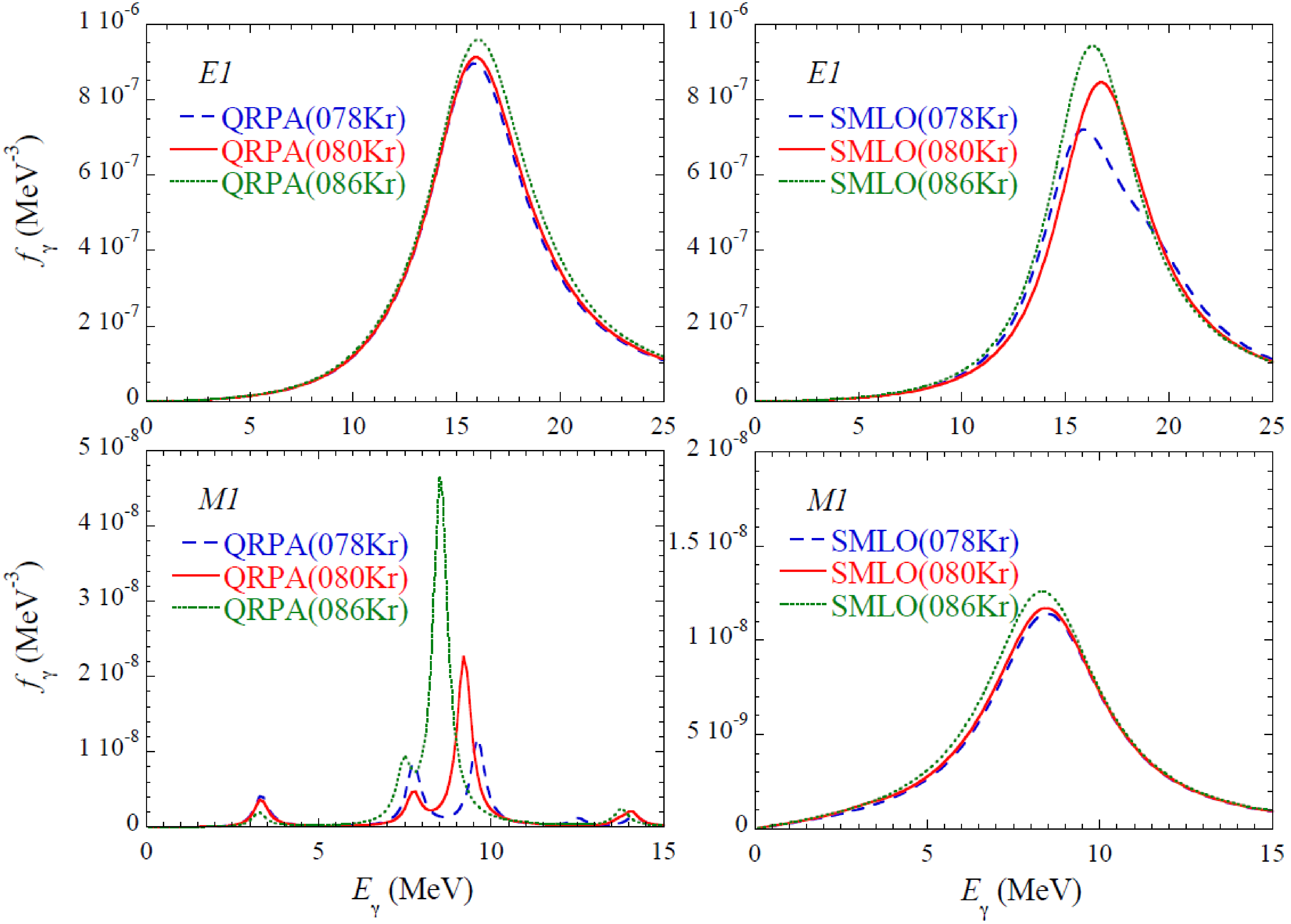

E1
QRPA(078Kr)
QRPA(080Kr)
QRPA(086Kr)
SMLO(078Kr)
SMLO(080Kr)
SMLO(086Kr)
M1
QRPA(078Kr)
QRPA(080Kr)
QRPA(086Kr)
SMLO(078Kr)
SMLO(080Kr)
SMLO(086Kr)
f_γ (MeV^{-3})
E_γ (MeV)
1 10^{-6}
8 10^{-7}
6 10^{-7}
4 10^{-7}
2 10^{-7}
5 10^{-8}
4 10^{-8}
3 10^{-8}
2 10^{-8}
1 10^{-8}
1.5 10^{-8}
5 10^{-9}

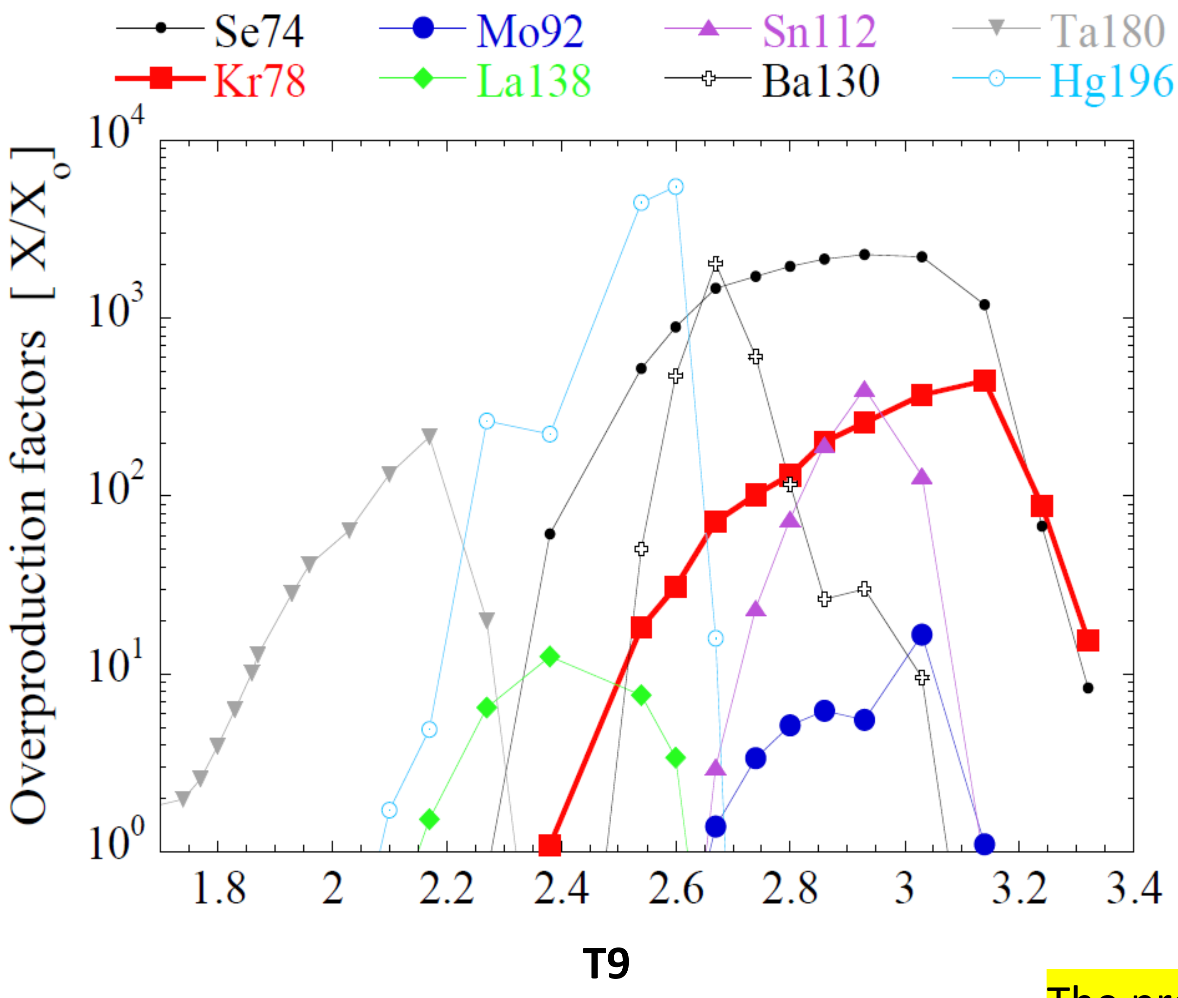

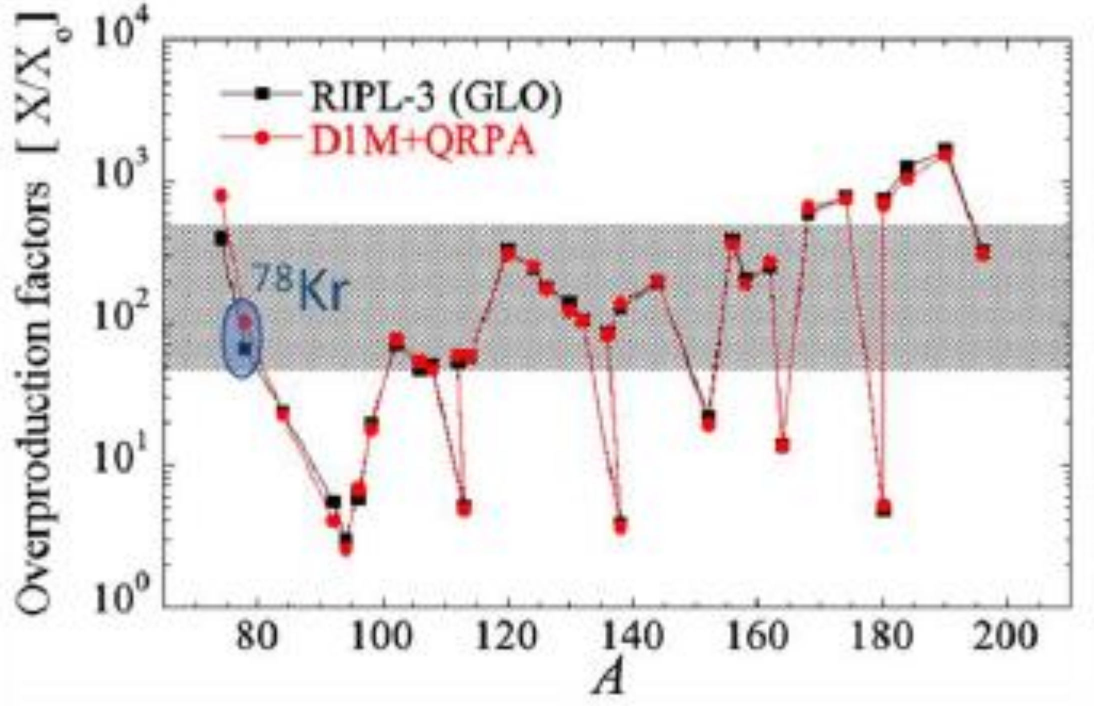

The production of the ^{78}Kr via the path ^{80}Kr(γ,n)^{79}Kr(γ,n)^{78}Kr is increased by 54%, while the (γ,n) destruction of ^{80}Kr is increased by a factor of 2.6 at *T* = 3 GK **when using the D1M+QRPA γSf model comparative to the GLO γSF model**.

PHOTONUCLEAR REACTIONS

$$\sigma_\gamma = \sigma_{\gamma\gamma} + \sigma_{\gamma\gamma'} \longrightarrow f(E_\gamma) = \frac{1}{3(\pi\hbar c)^2} \cdot \frac{\sigma_\gamma}{E_\gamma}$$

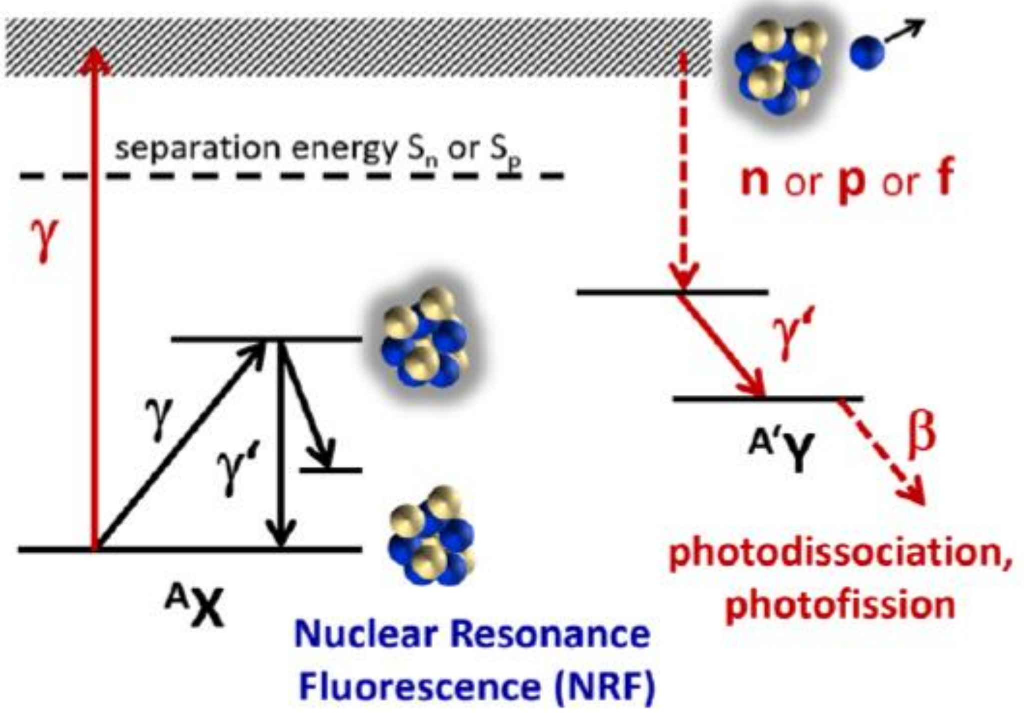

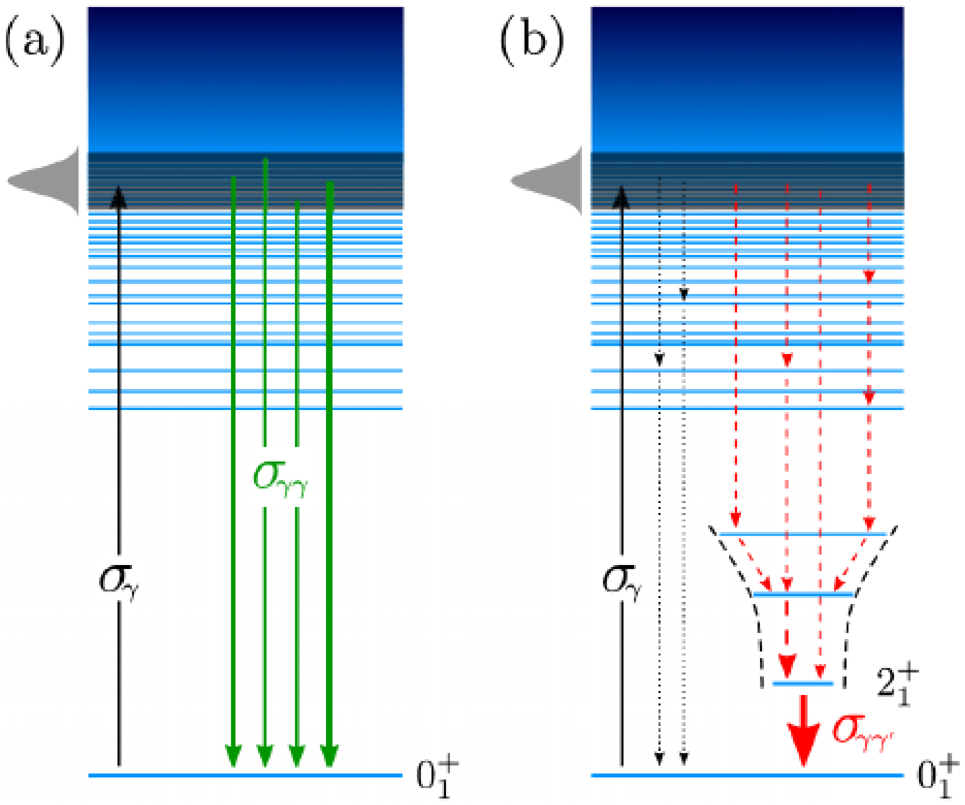

A. Zilges, D.L. Balabanski, J. Isaak, N. Pietralla, Prog. Part. Nucl. Phys. **122** (2022) 103903.

Parity and Spin Measurements with a Linearly Polarized Photon Beam

Dipole

E1

$0^+ \rightarrow 1^- \rightarrow 0^+$

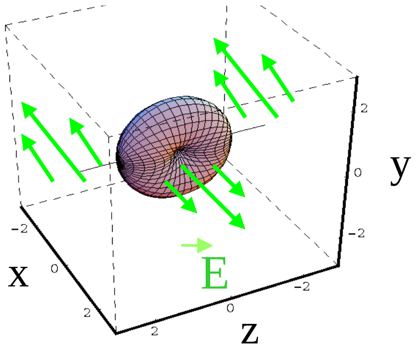

M1

$0^+ \rightarrow 1^+ \rightarrow 0^+$

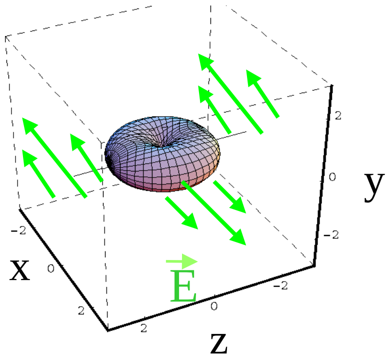

Quadruple

E2

$0^+ \rightarrow 2^+ \rightarrow 0^+$

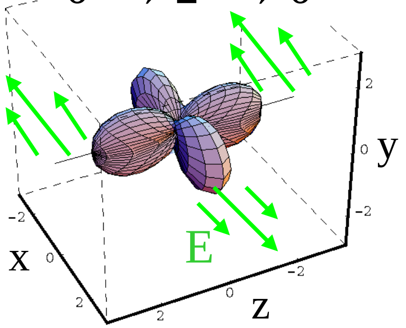

M2

$0^+ \rightarrow 2^- \rightarrow 0^+$

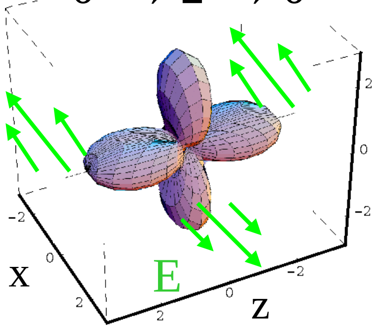

Azimuthal distribution

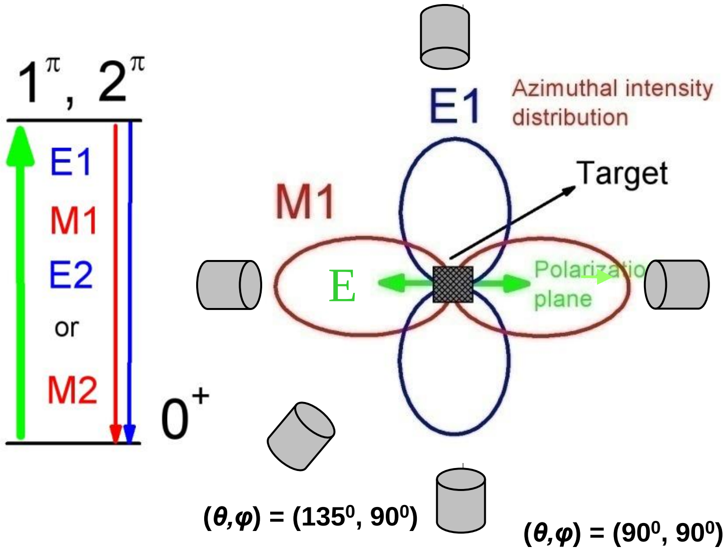

$$\Sigma = \frac{W(90^o,0^o) - W(90^o,90^o)}{W(90^o,0^o) + W(90^o,90^o)}$$

$$= \pi = \begin{cases} +1 & \text{for } J^\pi = 1^+, 2^+ \\ -1 & J^\pi = 1^-, 2^- \end{cases}$$

Experimental Asymmetry = 0.96

N. Pietralla, at al. PRL **88** (2002) 012502; A. Tonchev, NIM **B 241** (2005) 51474

NRF Experimental Setup at HγGS

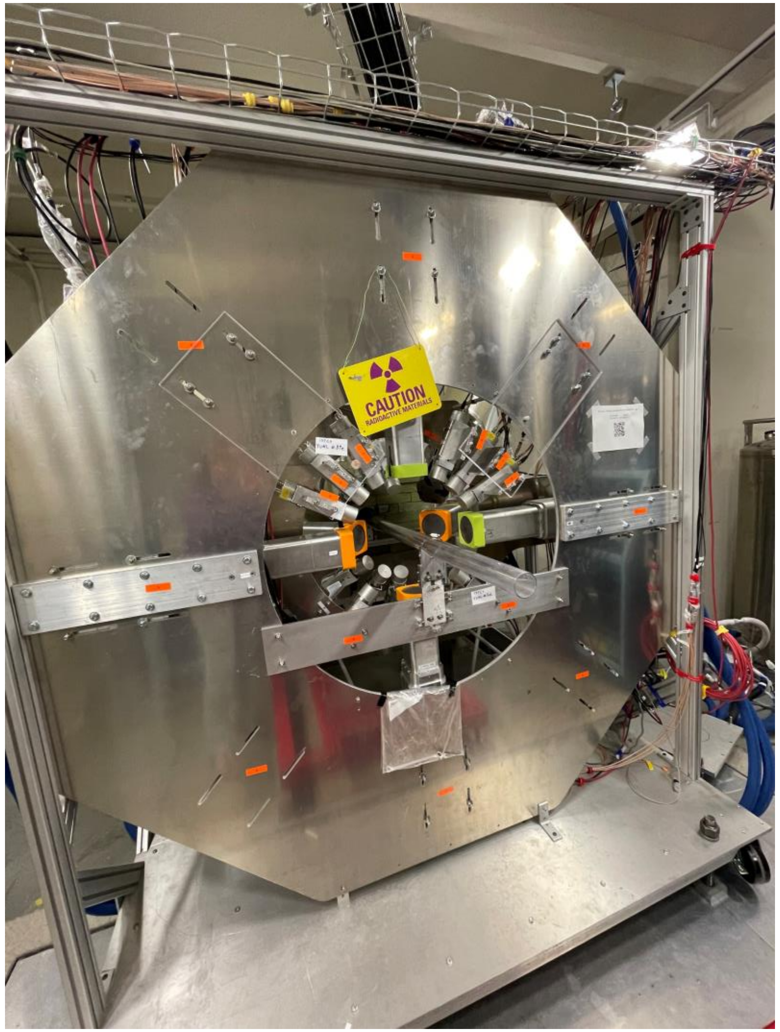

Clover array

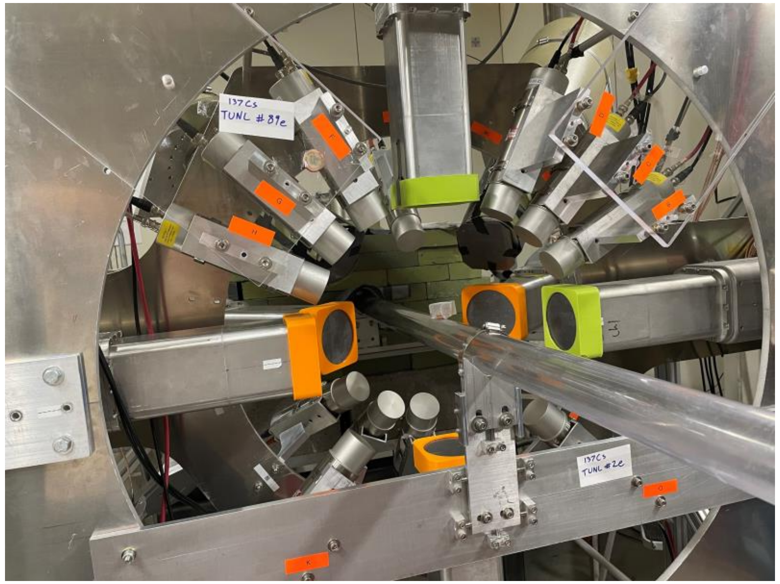

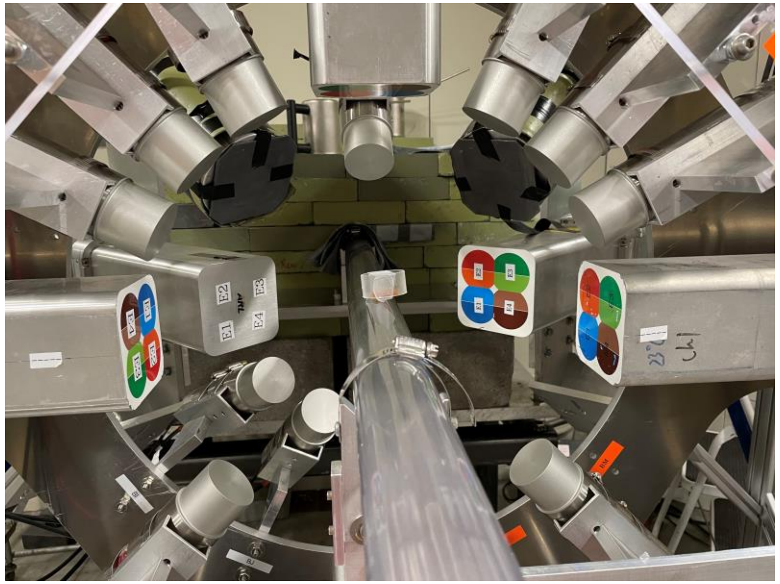

Target gas cell and target holder

Photon beam flux measurement

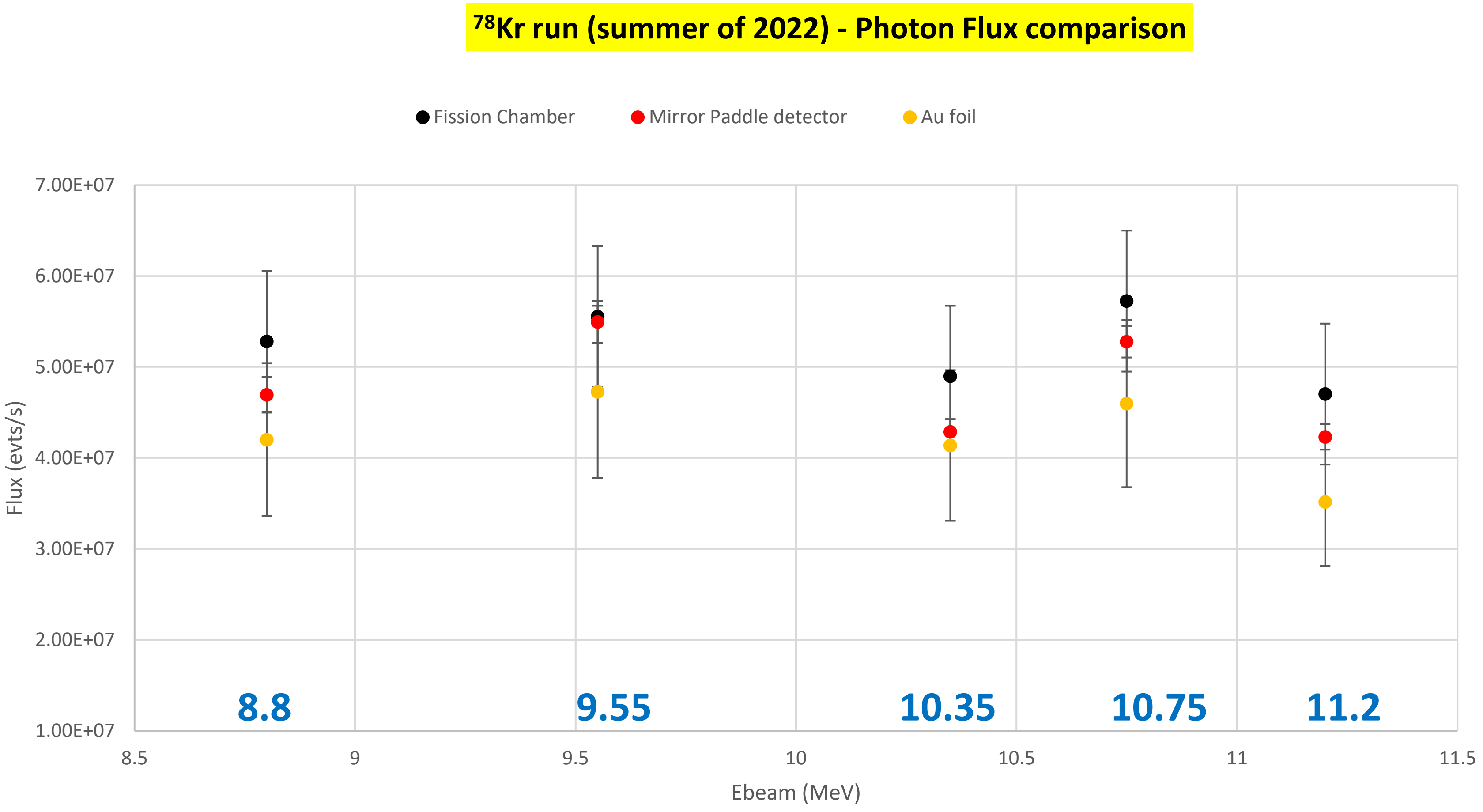

Photon Beam Energies (MeV) for our NRF measurements:

6.40, 6.65, 6.95, 7.20, 7.28, 7.50, 7.80, 8.15, 8.45, **8.80**, 8.92, 9.15, **9.55**, 9.95, **10.35, 10.75, 11.20**

$S_n(^{78}Kr)$ = 12.1 MeV

$S_n(^{80}Kr)$ = 11.5 MeV

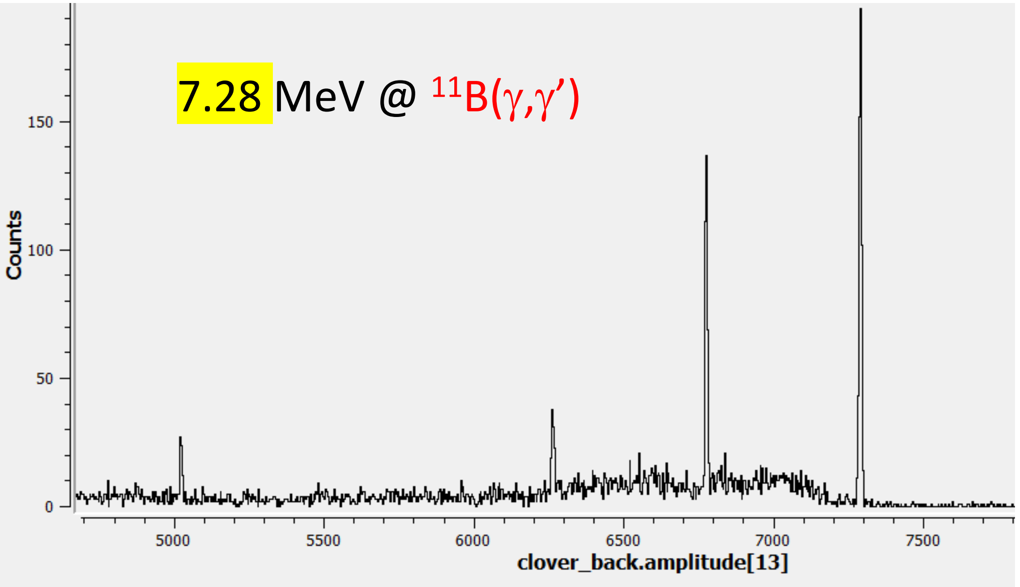

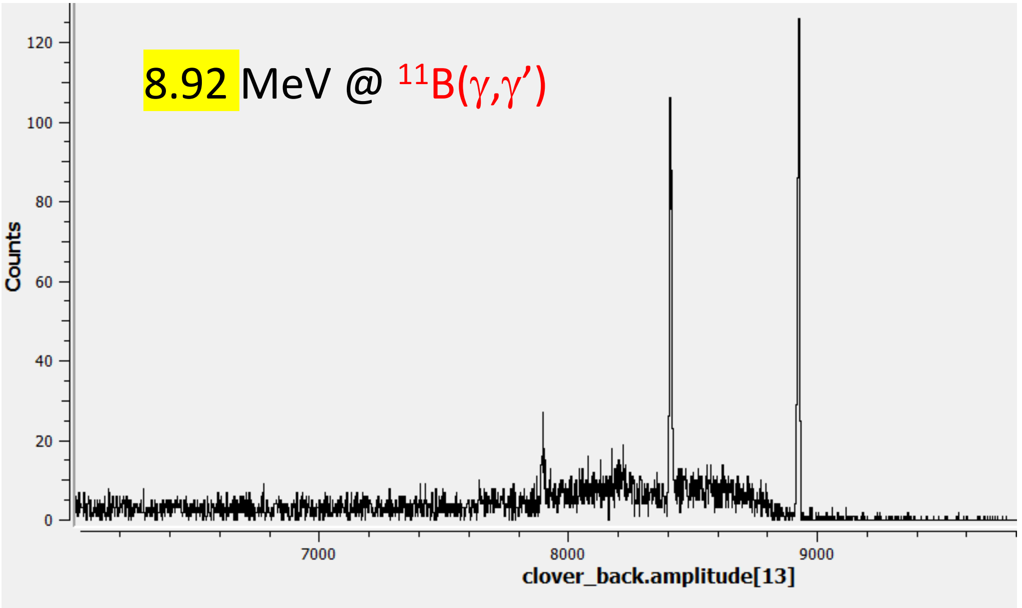

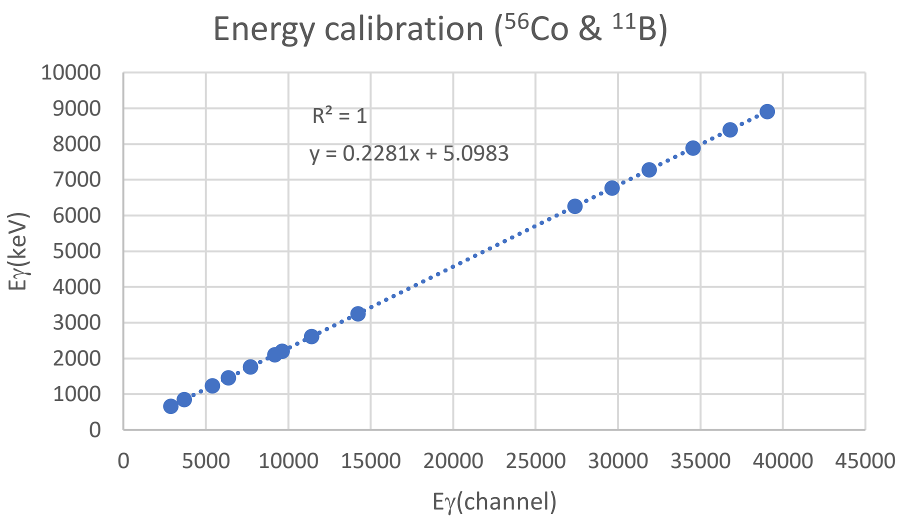

^{80}Kr NRF measurements (July 2023)

6.4 MeV @ ^{56,54}Fe(γ,γ') & **^{80}Kr(γ,γ')**

target: stainless-steel cell with **^{80}Kr**

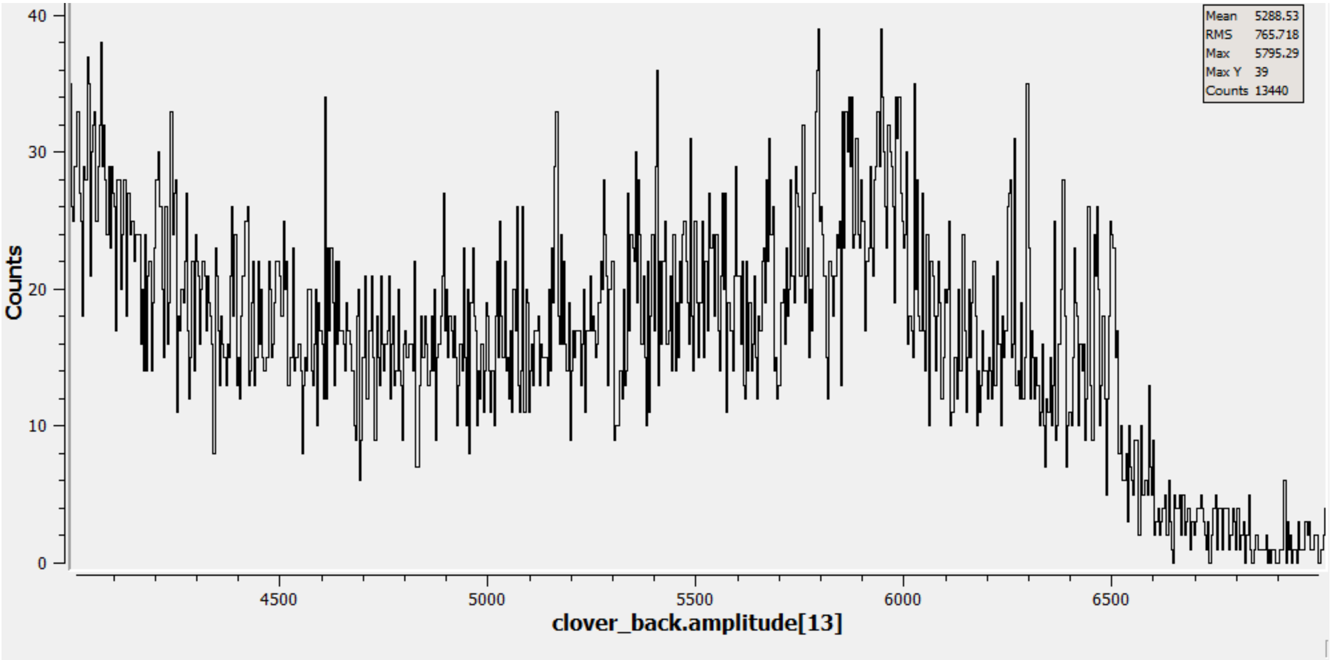

6.4 MeV @ ^{56,54}Fe(γ,γ')

target: stainless-steel **empty cell**

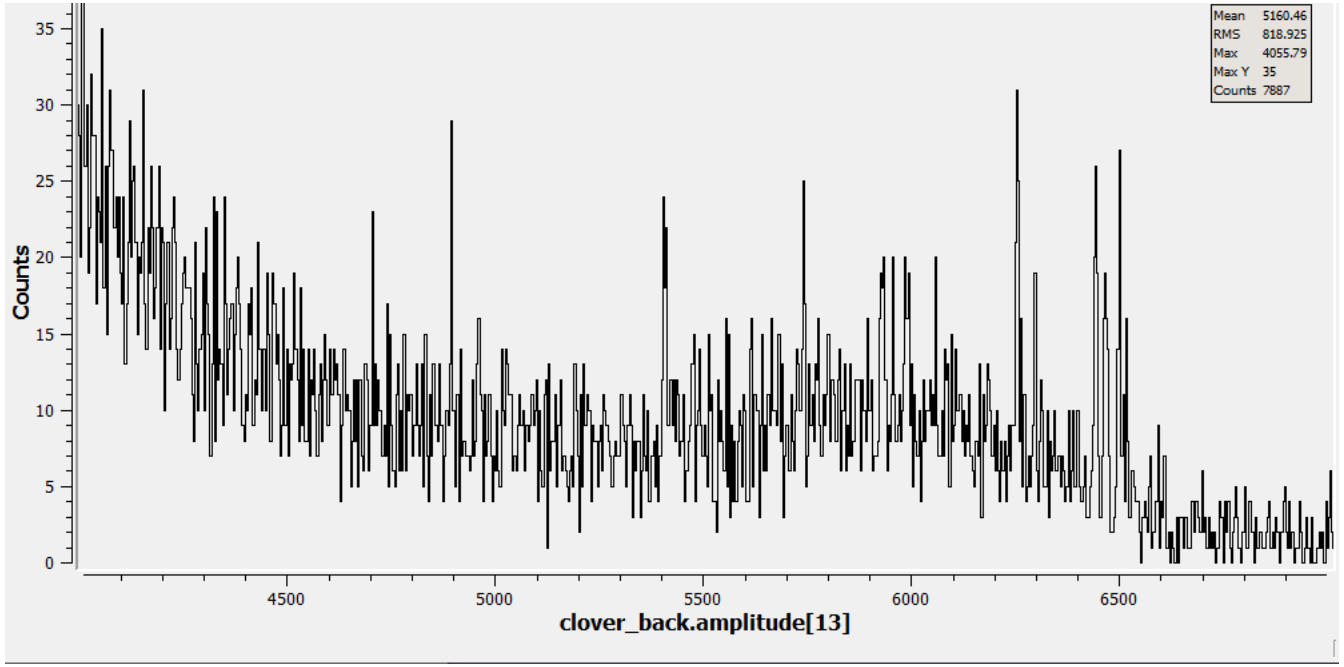

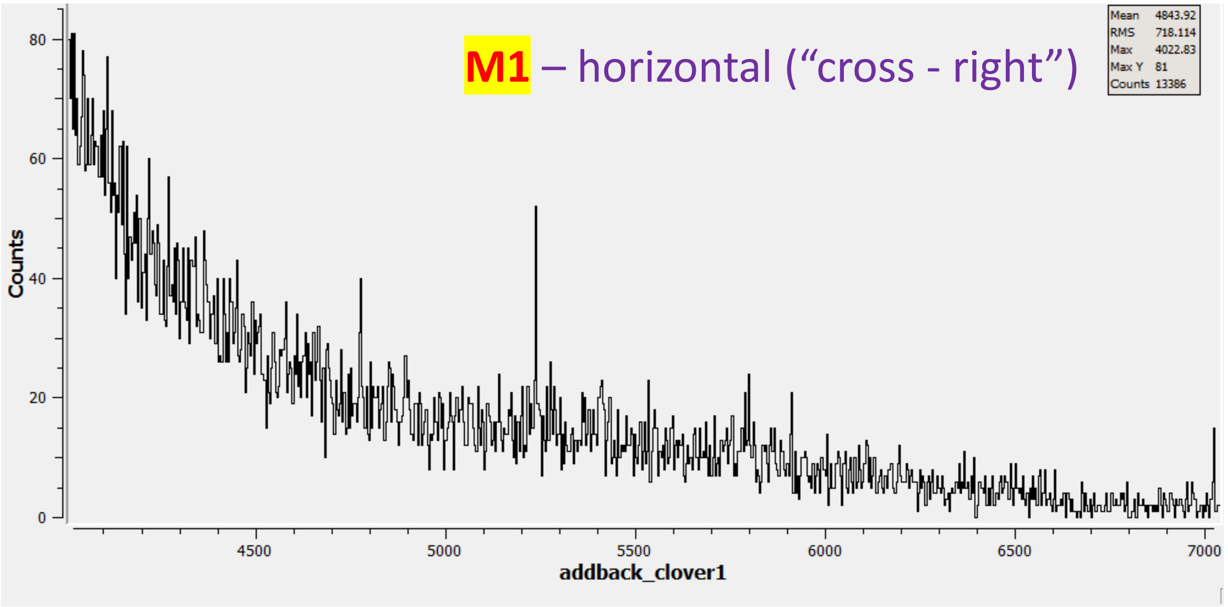

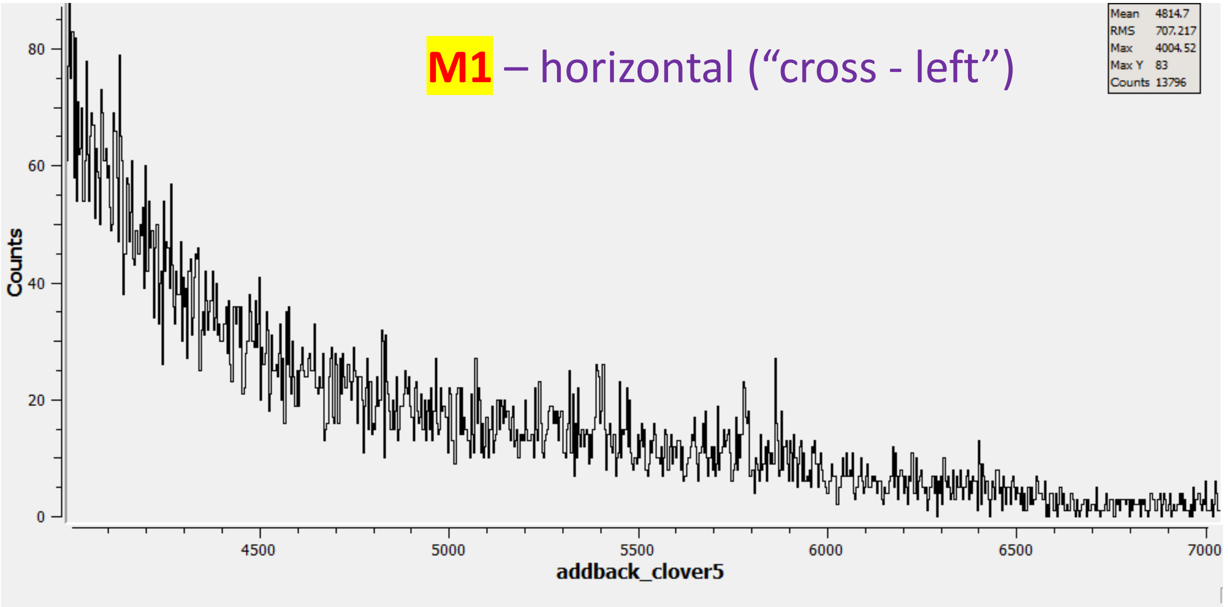

6.4 MeV @ $^{56,54}Fe(\gamma,\gamma')$ & $^{80}Kr(\gamma,\gamma')$

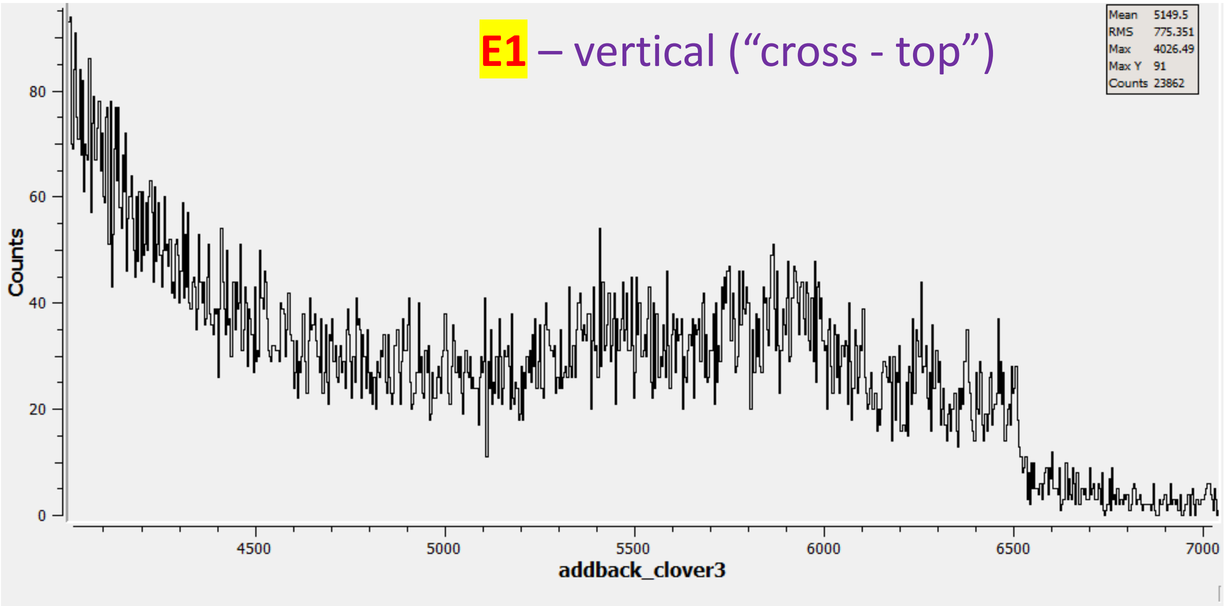

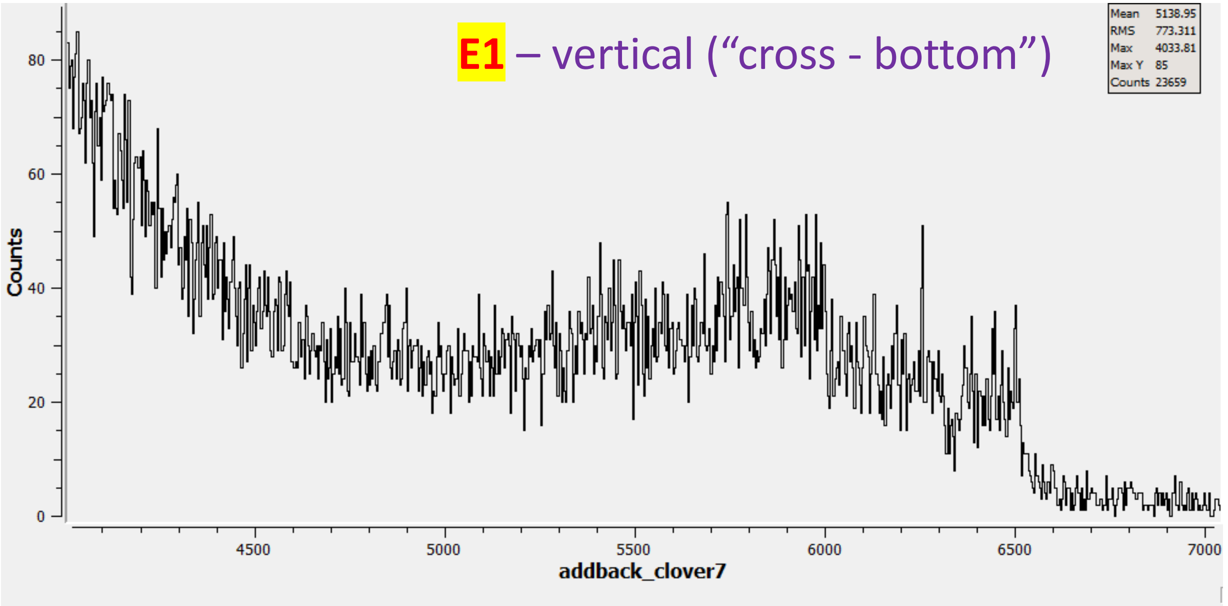

^{80}Kr NRF measurements (July 2023)

11.2 MeV @ ^{56,54}Fe(γ,γ') & **^{80}Kr(γ,γ')**

target: stainless-steel cell with **^{80}Kr**

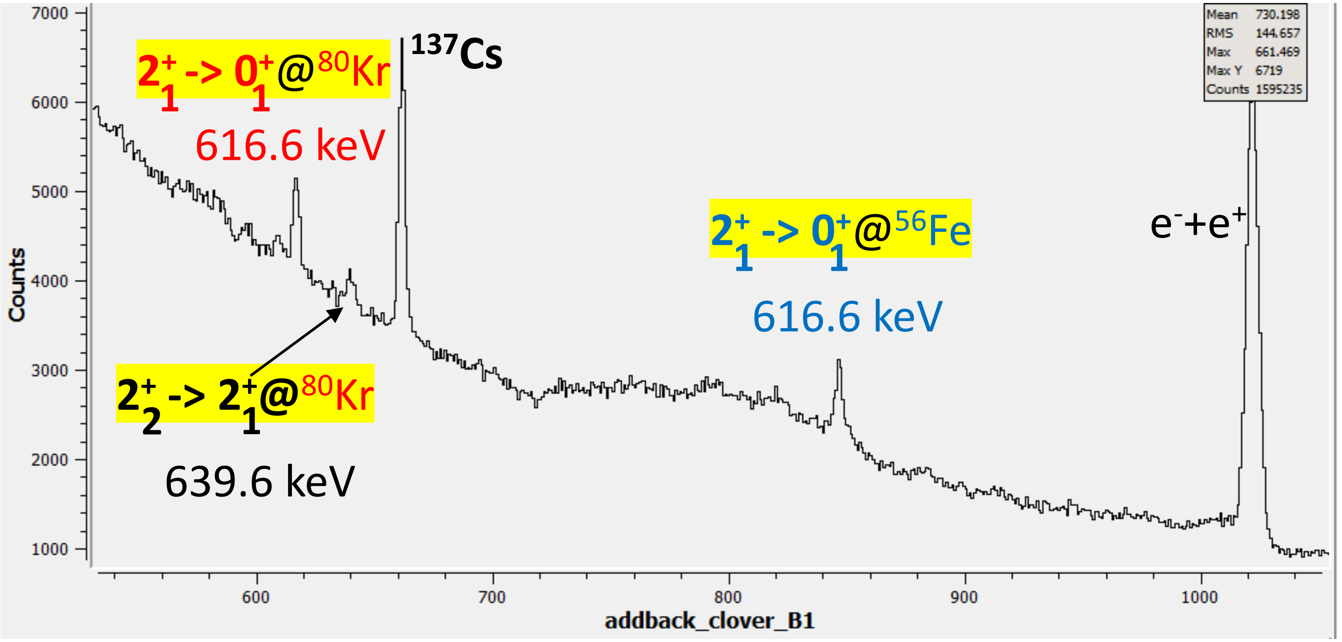

Data analysis in progress: **stay tuned**

Exploring the Origin of the Rarest Stable Isotopes via Photon-Induced Activation Studies at the Madison Accelerator Laboratory (MAL)

- James Madison University is an R2 university located in Harrisonburg, VA (in the beautiful Shenandoah Valley)
- Dept. of Physics and Astronomy is an undergraduate-only department
  - The department acquired **a medical electron linear accelerator (linac)** and an **X-ray imaging machine** from the former Cancer Therapy Center of the Rockingham Memorial Hospital.
  - In March **2018**, MAL became **officially licensed for operations** by the VA Dept. of Health
  - In September **2022**, MAL **joined ARUNA**

MAL mission is two-fold:

- Our **research-focused mission** is to repurpose and transform an "off-the-shelf" medical electron linear accelerator, originally used for clinical operations, into a multidisciplinary user-research facility available for all JMU faculty and students as well as for other higher-education institutions and research facilities in Virginia and beyond.
- Our **education-focused mission** is to forge collaborations between the physics, nuclear engineering and health science departments across the state of Virginia and beyond that focus on the development of a broad educational curriculum in applied photon science and accelerator or medical physics.

MAL (medical) electron linac – overview of its capabilities

- **Siemens Magnetron-based linac (3 GHz RF frequency)**
  - Dual Photon Beam (6 & 15 MV)
  - Multi-Energy Electron Beams (5, 7, 8, 10, 12, and 14 MeV)
- **Electron Beam Characteristics:**
  - Pulsed 3 μs beam at 100-300 Hz pulse repetition frequencies
  - Beam current: 0.1 – 10 mA avg, 0.15-1.5 A peak
- **Bremsstrahlung Target:** Tungsten
- **Dose rate:** ~3 Gy/min (photons), ~9 Gy/min (electrons) at isocenter
- **Beam profile:** up to 40 cm x 40 cm flat field at isocenter (reduceable with collimators)

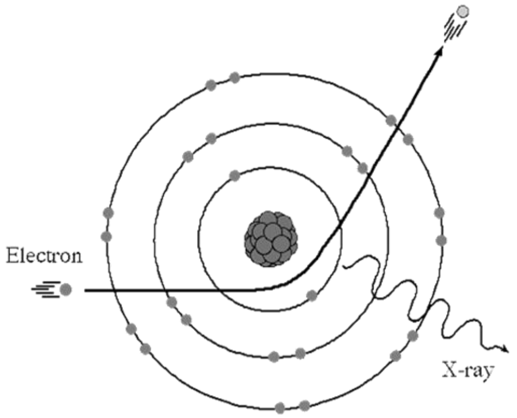

- **Associated Instrumentation:**
  - Suite of HPGe detectors w/ rel. efficiencies up to 60%, ultra-low background shielding
  - Suite of NaI(Tl) detectors with analog/digital base & LaBr3 detectors with digital base
  - Silicone surface-barrier detectors with fast/slow preamplifiers
  - Standalone DAQ systems (*i.e.*, Genie 2000 (Mirion), CAEN DT5725S digitizer)

Check out MAL website for more details: **https://sites.lib.jmu.edu/mal**

MAL Madison Accelerator Laboratory
Physics and Astronomy • James Madison University

ARUNA
Association for Research at University Nuclear Accelerators

Exploring the origin of *p*-nuclei via photon-induced activation studies @ MAL

- Measurements of ground state reaction rates for photo-neutron reactions relevant to the *p*-process nucleosynthesis
- Our objective is to compare experimental data to calculated ground-state reaction rates and cross sections in Hauser-Feshbach statistical reaction models
- *The ultimate goal here is to improve the knowledge of the dipole γ-strength functions*

The reaction rate for a photodisintegration reaction

$$\lambda(T)=\int_0^\infty c\, n_\lambda^{Planck}(E,T)\,\sigma(E)\,dE$$

$$n_\gamma^{Planck}(E,T)=\left(\frac{1}{\pi}\right)^2\left(\frac{1}{\hbar c}\right)^3\frac{E^2}{\exp(E/kT)-1}$$

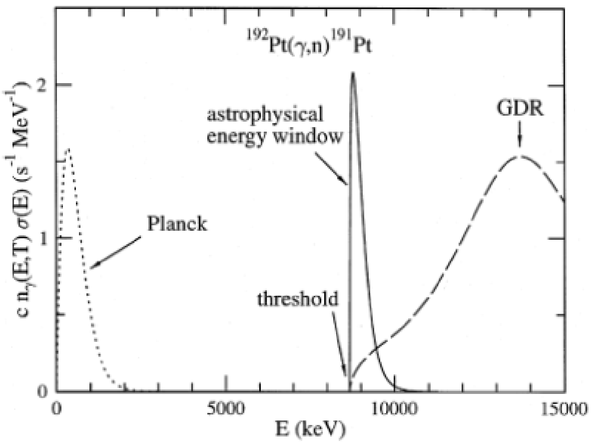

P. Mohr et al. (Phys. Lett. B 488, (2000))

'The superposition method'

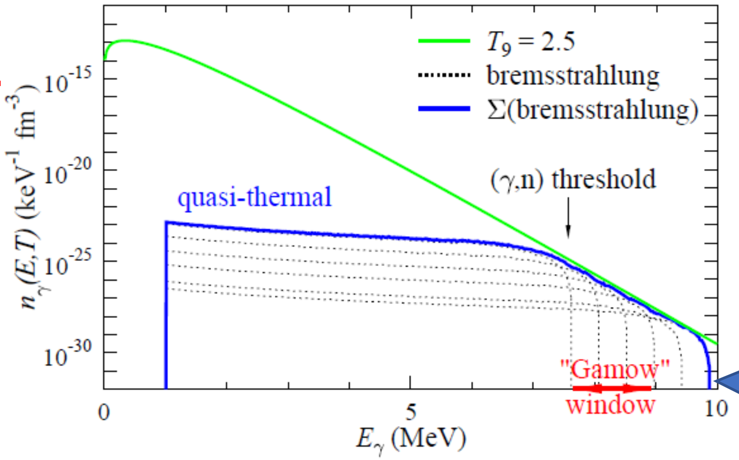

$$c\,n_\gamma^{Planck}(E,T)\approx\sum_i a_i(T)\,\Phi_\gamma^{brems}(E,E_{\max,i})$$

$$\lambda^{gs}_{(\gamma,n)}(T)\approx\sum_i a_i(T)\int_{E_{thr}}^{E_{\max,i}}\Phi_\gamma^{brems}(E,E_{\max,i})\,\sigma_{(\gamma,n)}(E)\,dE$$

$$\lambda^{gs}_{(\gamma,n)}(T)\approx\sum_i a_i(T)\,I_{\sigma(\gamma,n),i}$$

$$\gamma+{}^{A}X\rightarrow{}^{A-1}X^{*}+n$$

$$A_\gamma=N_T\varepsilon_\gamma I_\gamma\,p\,\frac{t_{life}}{t_{real}}\,\frac{\left(1-e^{-\lambda t_{irr}}\right)}{\lambda t_{irr}}\,e^{-\lambda t_{cool}}\left(1-e^{-\lambda t_{meas}}\right)I_{\sigma(\lambda,n)}$$

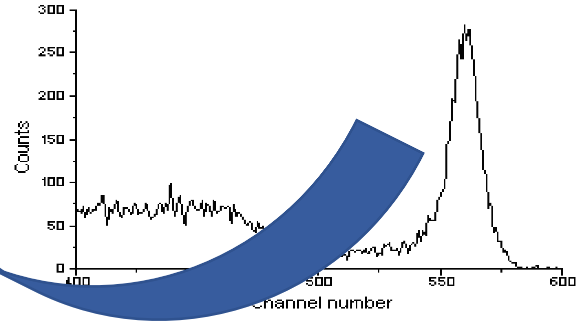

❖ Measurements of (γ,n) reaction rates on stable proton-rich nuclei with reaction threshold around 12 MeV!

$^{74}Se(\gamma,n)^{73}Se$ — $T_{1/2} = 7.15h$

$^{78}Kr(\gamma,n)^{77}Kr$ — $T_{1/2} = 74.4m$

$^{84}Sr(\gamma,n)^{83}Sr$ — $T_{1/2} = 32.41m$

$^{80}Kr(\gamma,n)^{79}Kr$ — $T_{1/2} = 35.04h$

$^{64}Zn(\gamma,n)^{63}Zn$ — $T_{1/2} = 38.47m$

$^{70}Ge(\gamma,n)^{69}Ge$ — $T_{1/2} = 39.05h$

$^{86}Sr(\gamma,n)^{85}Sr$ — $T_{1/2} = 64.85d$

$^{90}Zr(\gamma,n)^{89}Zr$ — $T_{1/2} = 78.4\ h$

This work is supported by the National Science Foundation through the Grant No. Phys - 1913258

Determination of bremsstrahlung endpoint energy @ MAL

- Developing deuteron breakup measurements similar to ELBE facility

- Irradiate deuteron breakup target with γ and measure proton energy

$$^{2}H(\gamma, p)n$$

$$E_p[MeV] = \frac{E_\gamma - 2.22}{2}$$

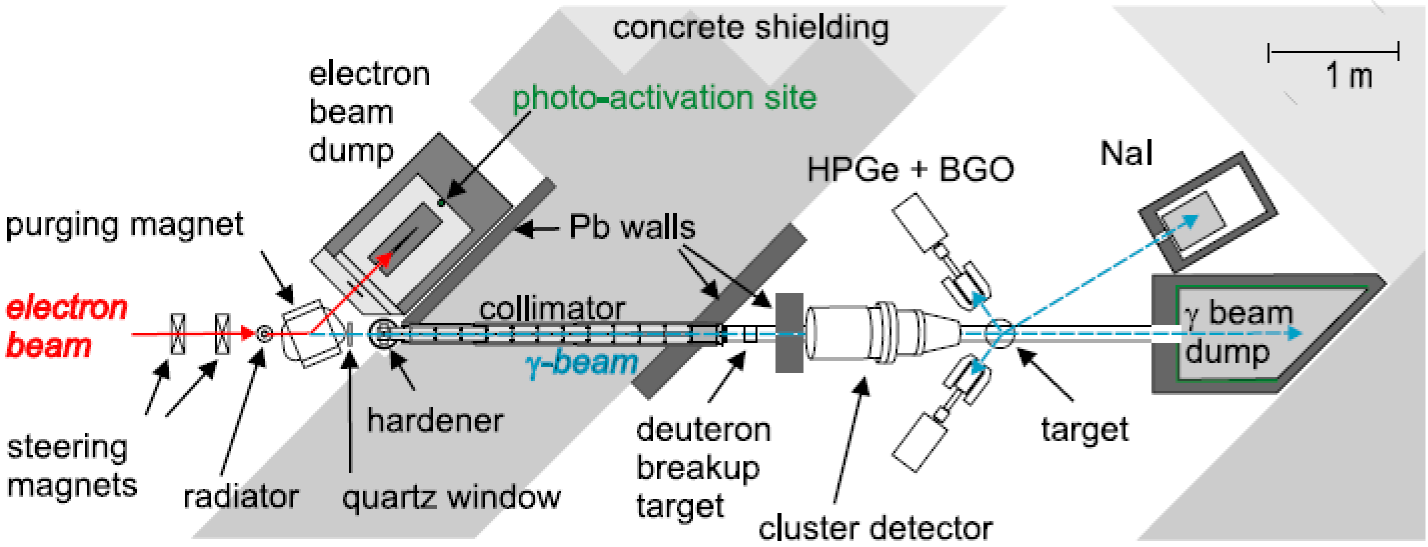

Figure 1. Bremsstrahlung facility and experimental area for photon-scattering and photo-dissociation experiments at the ELBE accelerator.

Wagner *et al*. (J. Phys. G 31 (2020))

➢ **15 MeV @ MAL** => 6.39 MeV (max proton energy)

Photodisintegration of deuteron @ ELBE facility

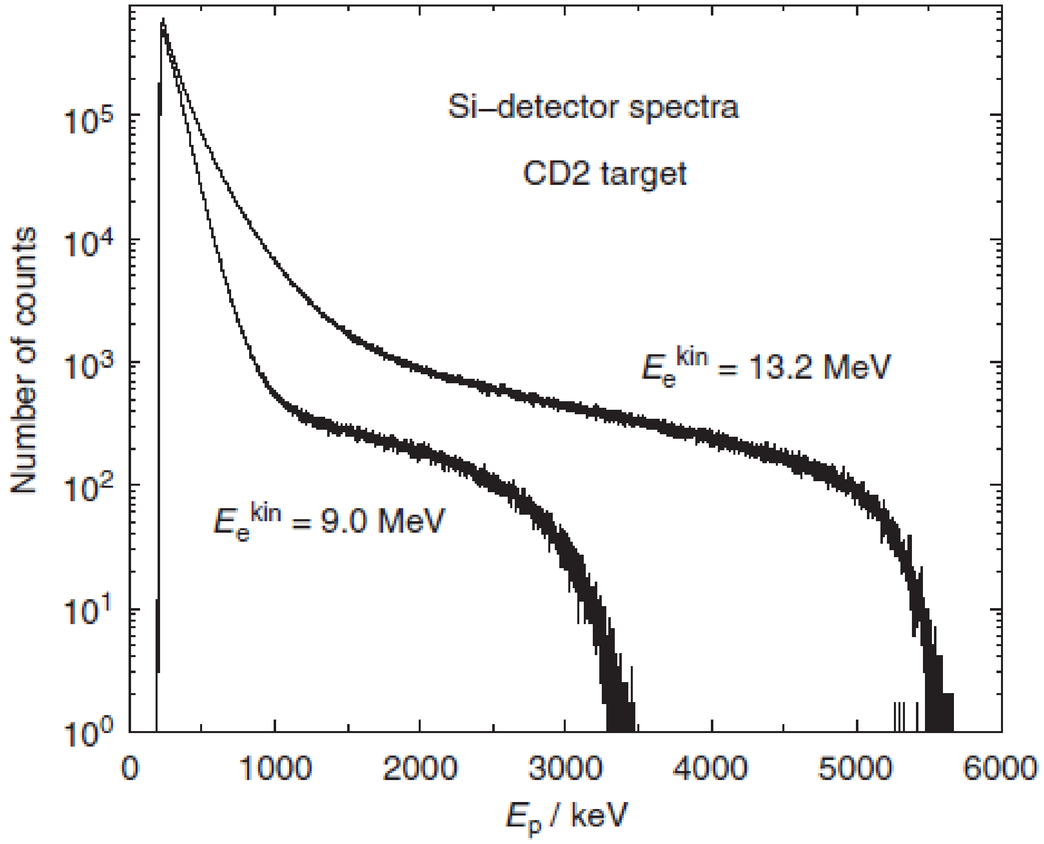

R. Schwengner et al., NIM A555 (2005) 211

C. Nair et al., Phys. Rev. C 78, 055802 (2008)

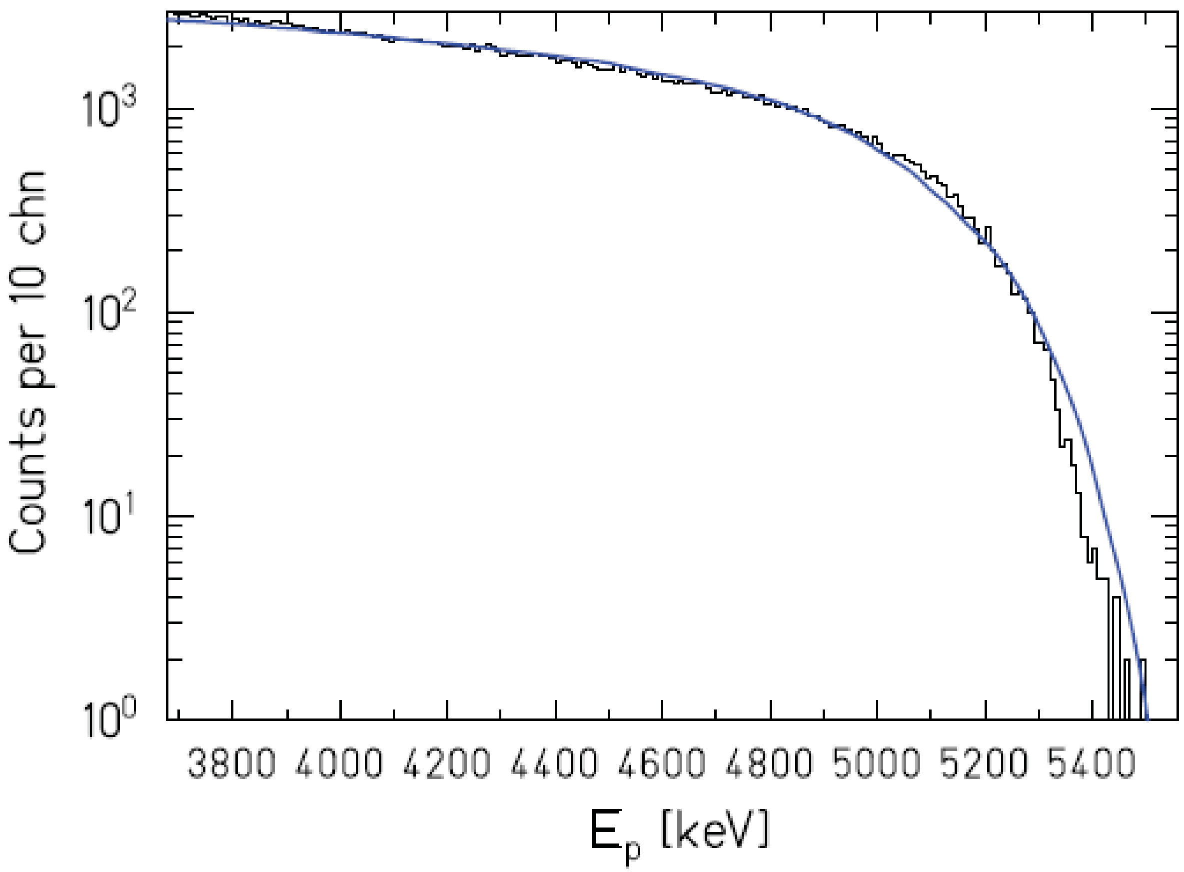

Determination of bremsstrahlung endpoint energy @ MAL (cont’d)

- Have acquired deuteron target and assembling shielded beam line

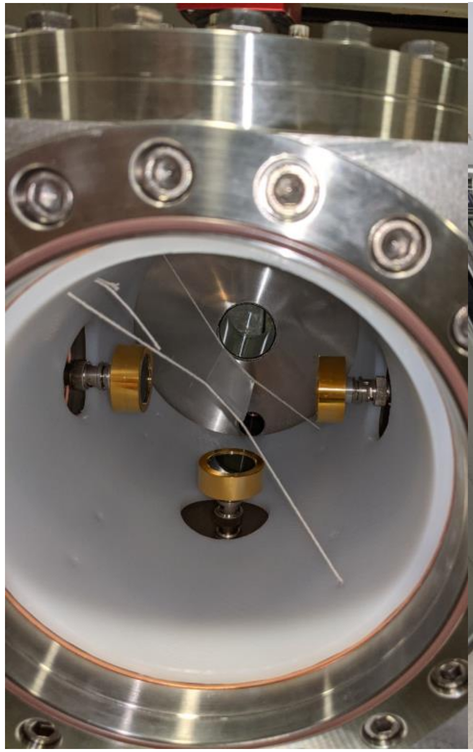

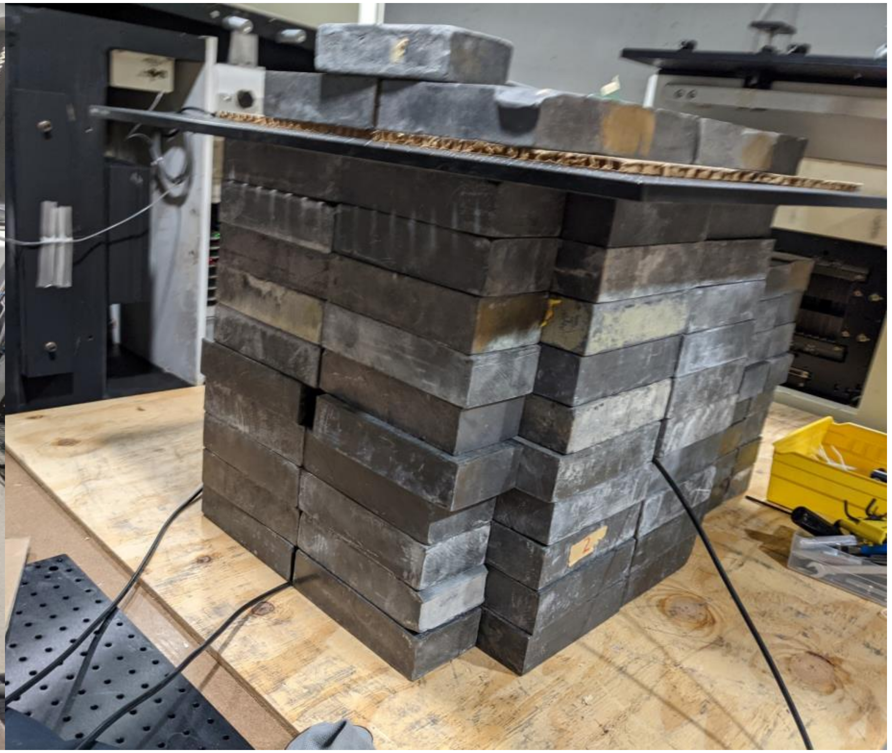

Determination of bremsstrahlung endpoint energy @ MAL (work in progress)

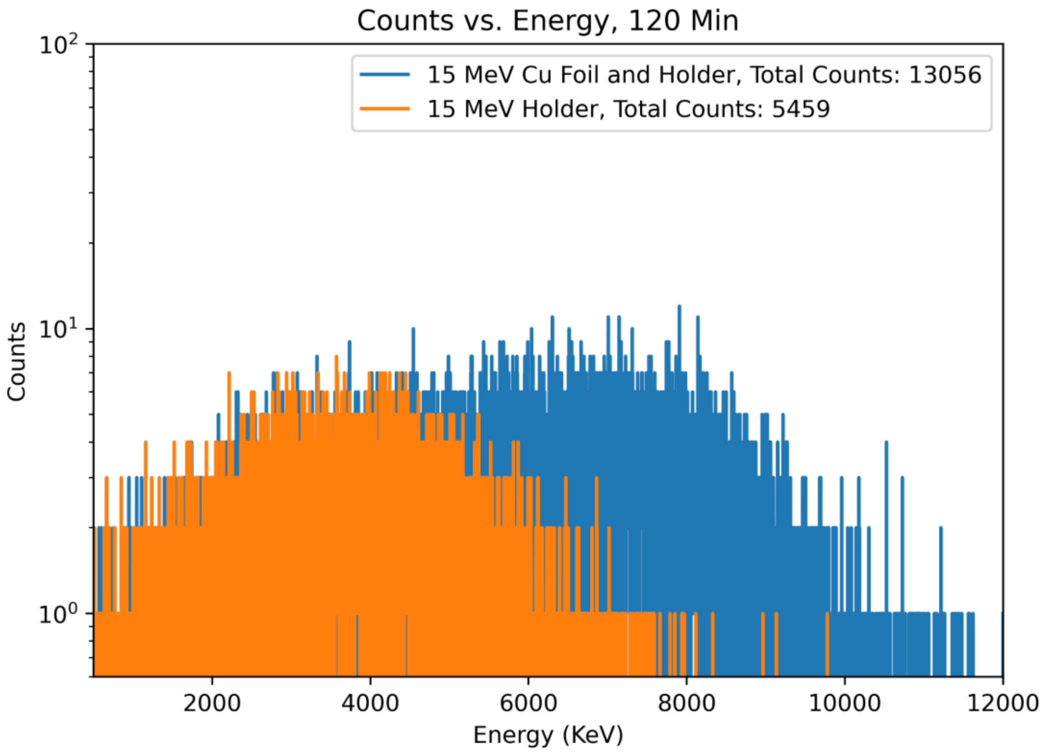

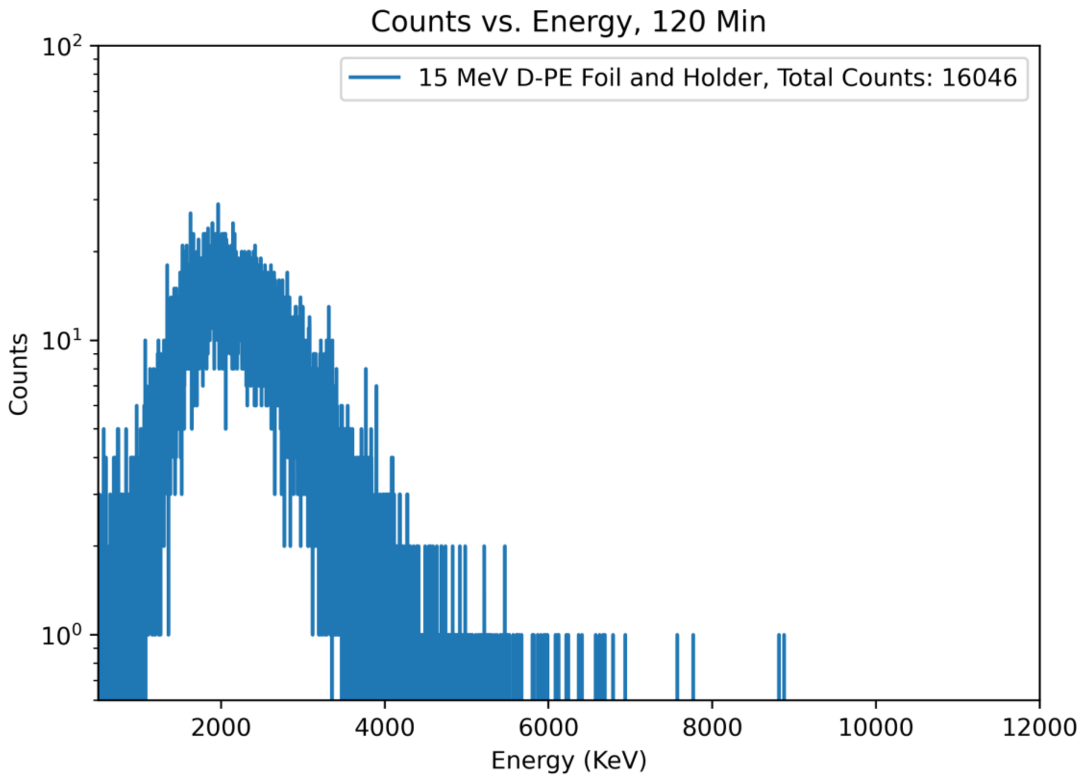

Cu foil: ^{63}Cu (70%; Sp = 6 MeV) & ^{65}Cu (30%; Sp = 7.5 MeV)

- **15 MeV @ MAL** => 9 MeV (max proton energy)
- **15 MeV @ MAL** => 6.39 MeV (max proton energy)

Half-Life Measurements @ MAL (published results)

$$\lambda^{gs}_{(\gamma,n)}(T) \approx \sum_i a_i(T) I_{\sigma_{(\gamma,n)},i}$$

$$\gamma + {}^{A}X \rightarrow {}^{A-1}X^{*} + n$$

$$A_\gamma = N_T \varepsilon_\gamma I_\gamma p \frac{t_{life}}{t_{real}} \frac{\left(1-e^{-\lambda t_{irr}}\right)}{\lambda t_{irr}} e^{-\lambda t_{cool}} \left(1-e^{-\lambda t_{meas}}\right) I_{\sigma(\lambda,n)}$$

High-precision measurements of half-lives for ^{69}Ge, ^{73}Se, ^{83}Sr, ^{85m}Sr, and ^{63}Zn radionuclides relevant to the astrophysical *p*-process via photoactivation at the Madison Accelerator Laboratory

T. A. Hain[1] · S. J. Pendleton[1] · J. A. Silano[2] · A. Banu[1]

Received: 3 September 2020 / Accepted: 31 December 2020

Abstract
The ground state half-lives of ^{69}Ge, ^{73}Se, ^{83}Sr, ^{63}Zn, and the half-life of the 1/2$^-$ isomer in ^{85}Sr have been measured with high precision using the photoactivation technique at an unconventional bremsstrahlung facility that features a repurposed medical electron linear accelerator. The *γ*-ray activity was counted over about 6 half-lives with a high-purity germanium detector, enclosed into an ultra low-background lead shield. The measured half-lives are: $T_{1/2}(^{69}\mathrm{Ge}) = 38.82 \pm 0.07$ (stat) ± 0.06 (sys) h; $T_{1/2}(^{73}\mathrm{Se}) = 7.18 \pm 0.02$ (stat) ± 0.004 (sys) h; $T_{1/2}(^{83}\mathrm{Sr}) = 31.87 \pm 1.16$ (stat) ± 0.42 (sys) h; $T_{1/2}(^{85m}\mathrm{Sr}) = 68.24 \pm 0.84$ (stat) ± 0.11 (sys) min; $T_{1/2}(^{63}\mathrm{Zn}) = 38.71 \pm 0.25$ (stat) ± 0.10 (sys) min. These high-precision half-life measurements will contribute to a more accurate determination of corresponding ground-state photoneutron reaction rates, which are part of a broader effort of constraining statistical nuclear models needed to calculate stellar nuclear reaction rates relevant for the astrophysical *p*-process nucleosynthesis.

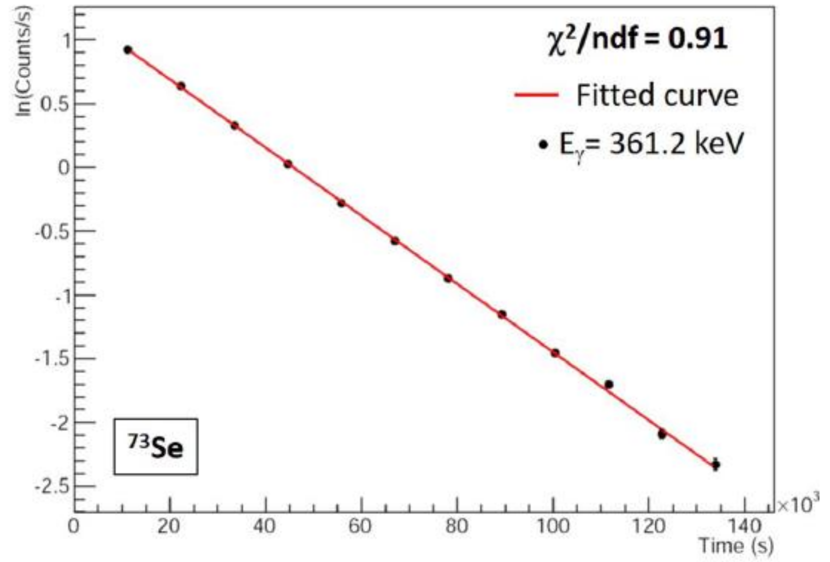

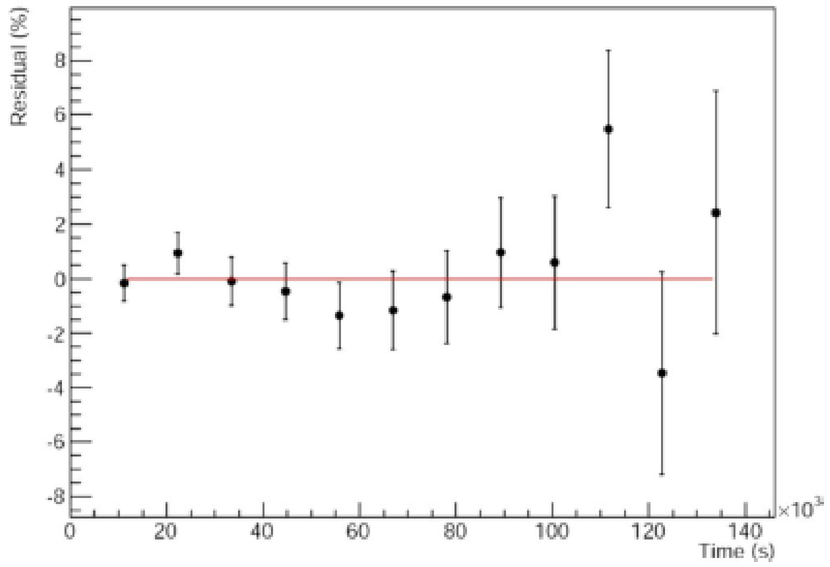

J. Radioanalytical and Nuclear Chemistry 32, 1113 (2021)

Half-Life Measurements @ MAL (preliminary results)

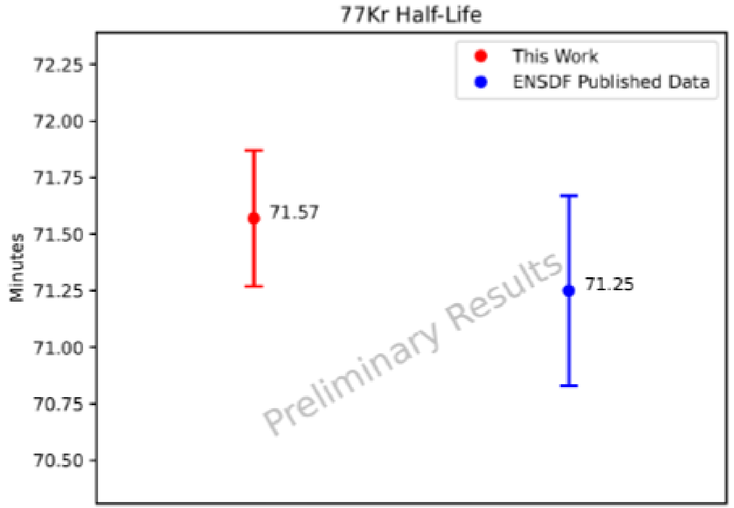

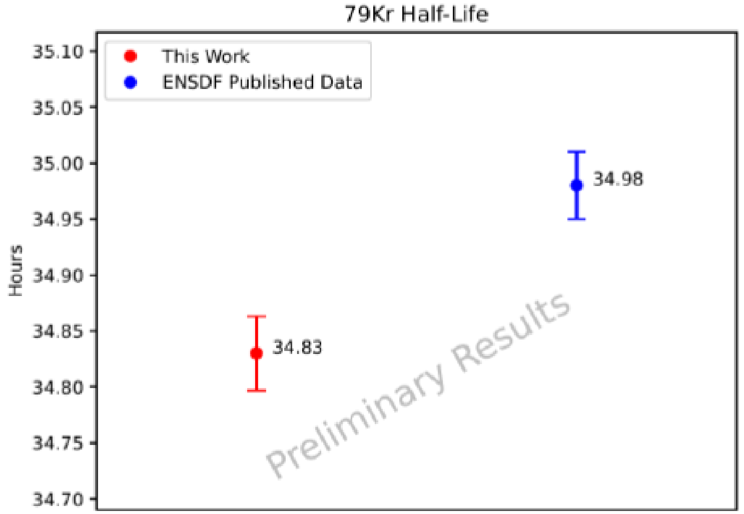

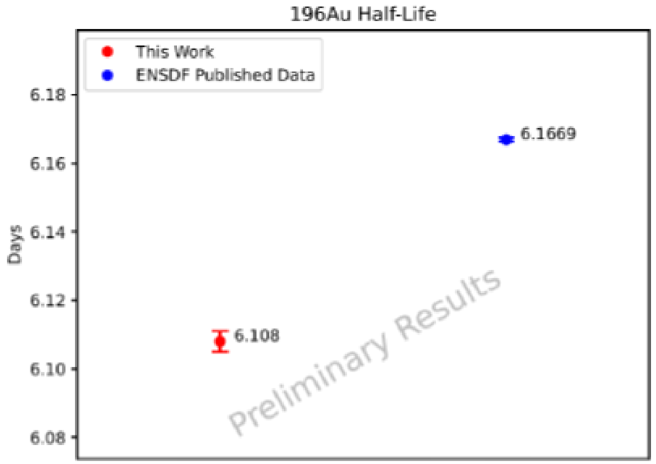

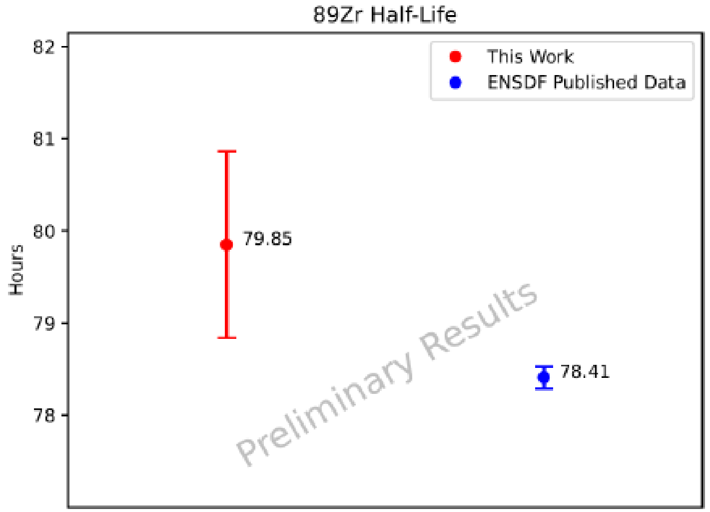

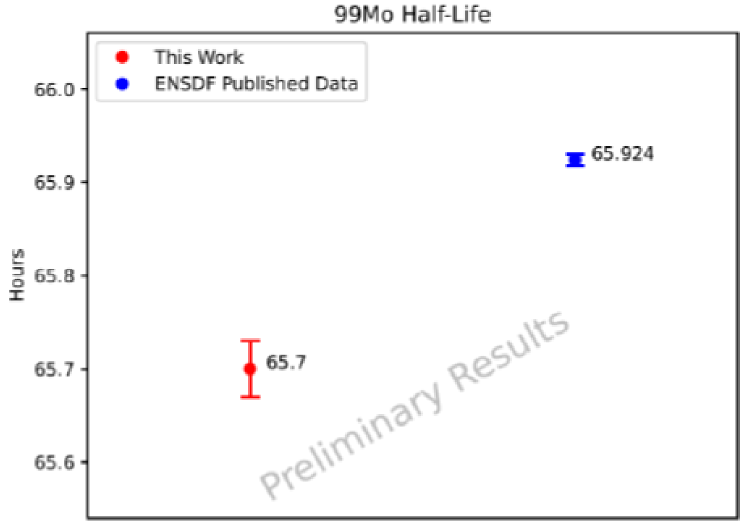

Acknowledgments

Research work for the ^{78,80}Kr(γ,γ') measurements is supported by the award no. DE-SC0021199

Research work for the ^{94}Mo(γ,n) and ^{90}Zr(γ,n) measurements was partially supported by the award no. 22662

The theoretical work for the ^{94}Mo(γ,n) and ^{90}Zr(γ,n) measurements was performed within the IAEA CRP on "Updating the Photonuclear Data Library and Generating a Reference Database for Photon Strength Functions" (F41032)

S. Goriely *et al.*, **Eur. Phys. J. A55, 172 (2019):** ***Reference Database for Photon Strength Functions***
T. Kawano *et al.*, **Nucl. Data Sheets 163, 109 (2020):** ***IAEA Photonuclear Data Library 2019***

Thank you for your attention!